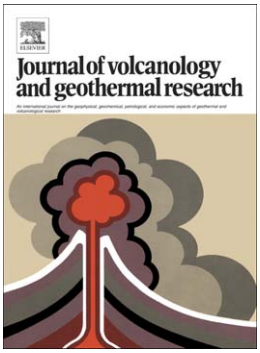

Primary Igneous Anhydrite: Progress since its Recognition in the 1982 El Chichón Trachyandesite

James F. Luhr

PII: S0377-0273(08)00161-3
DOI: doi: 10.1016/j.jvolgeores.2008.02.016
Reference: VOLGEO 3961

To appear in: *Journal of Volcanology and Geothermal Research*

Accepted date: 12 February 2008

Please cite this article as: Luhr, James F., Primary Igneous Anhydrite: Progress since its Recognition in the 1982 El Chichón Trachyandesite, *Journal of Volcanology and Geothermal Research* (2008), doi: 10.1016/j.jvolgeores.2008.02.016

Primary Igneous Anhydrite: Progress since its Recognition in the 1982 El Chichón Trachyandesite

James F. Luhr
Department of Mineral Sciences
Smithsonian Institution
P.O. Box 37012, NHB-119
Washington, D.C. 20013-7012, USA
Phone: 202-633-1802
Fax: 202-357-2476
E-mail: luhrj@si.edu

Abstract

Primary igneous anhydrite was first identified in 1982 El Chichón pumices. Analysis of the sulfur budget for the eruption provided compelling evidence that the pre-eruptive magma contained a significant gas phase at ~7 km depth in order to account for the "excess gas release" of ~5-9 million tons of SO_2 to the stratosphere by the eruption. Primary igneous anhydrite and a larger "excess gas release" of ~20 million tons of SO_2 were noted for the significantly larger eruption of Mount Pinatubo in 1991, for which a separate gas phase at ~7-9 km depth was also required by the sulfur budget. Pumices from both eruptions have mineral assemblages dominated by plagioclase and hornblende, with minor biotite, and show evidence for co-nucleation and mutual inclusions of anhydrite and apatite. Both magmas were also very water rich and highly oxidized, with oxygen fugacities ≥1 log unit above the synthetic Ni-NiO buffer. Furthering the similarities between these two eruptions, ion-microprobe analyses of sulfur isotopic compositions of anhydrites in pumices from El Chichón and Mount Pinatubo both showed that individual crystals are isotopically homogeneous, but inter-crystalline variations in $\delta^{34}S$ are well beyond analytical error.

This study reviews the history of thought regarding primary igneous anhydrite. Ten volcanic and plutonic analogues to the El Chichón and Mount Pinatubo magmas are discussed. All were similarly water-rich and highly oxidized magmas. Hornblende is the dominant mafic phenocryst in all but one plutonic example; in that case so much early anhydrite precipitated that no calcium remained to form hornblende. Biotite is very abundant in that exceptional plutonic case, and is present in six of the other examples with primary igneous anhydrite. Sphene is known as an indicator mineral of high magmatic oxygen fugacity; it was present in the 1982 El

Chichón pumices, and in 6 of the other anhydrite-bearing samples.

Hornblende and biotite phenocrysts are also characteristic of the intermediate-to-felsic plutonic rocks that typically host porphyry-Cu deposits. Such magmas are also known to be water rich and highly oxidized. A close spatial and petrogenetic connection exists between magmas with primary igneous anhydrite and magmatic-hydrothermal ore deposits.

Introduction

Anhydrite is an orthorhombic mineral with a nominally simple chemical formula of $CaSO_4$. It occurs in a wide range of geological environments, and has been involved in many new geological discoveries during the past three decades. Of those new discoveries, this paper will focus on primary igneous anhydrite, precipitated from silicate melts. Although anhydrite had been noted earlier in igneous rocks, the first recognition of unequivocal primary igneous anhydrite was in the trachyandesitic pumices erupted from El Chichón Volcano in 1982 (Luhr et al., 1984). After some general background on anhydrite occurrences in other rock types, the history of thought regarding anhydrite in igneous rocks will be reviewed along with its importance as an indicator of both high magmatic sulfur contents and high oxygen fugacities.

Anhydrite and its hydrated equivalent gypsum are most abundant on Earth and best known as major minerals in thick marine evaporite deposits (Warren, 1999; Spencer, 2000). The sulfate minerals that evaporate from seawater are known to have the same sulfur isotopic ratios as sulfate ions (SO_4^{2-}) in seawater. Thus, sedimentary anhydrite and gypsum have been used to track the sulfur isotopic composition ($\delta^{34}S$) of ocean water through geological time (Holser, 1977; Claypool et al., 1980; Bottrell and Newton, 2006). Minor sulfur-rich impact spherules

from the Cretaceous/Tertiary boundary clays have been interpreted as evidence that upper crustal limestone and anhydrite beds were among the target rocks at the Chicxulub crater in Mexico's northern Yucatán Peninsula (Izett, 1991; Bohor and Glass, 1995; Yang and Ahrens, 1998).

Formation of anhydrite also occurs where groundwater and sulfur-bearing hot magmatic systems are in contact. Examples include fumaroles at active volcanoes (Stoiber and Rose, 1974; Africano and Bernard, 2000; Rye, 2005; Zimbelman et al., 2005), deeper water-rock systems that are exploited for geothermal energy (Sasaki et al., 2003; Pape et al., 2005), still deeper systems where magmatic-hydrothermal ore deposits are formed (Field et al., 2005; Rye, 2005), and oceanic equivalents where hydrothermal vents build anhydrite-cemented chimneys and other hot ephemeral structures on the cold sea floor that survive only as long as they remain hot, a consequence of anhydrite's retrograde thermal solubility (Shikazono and Kusakabe, 1999; Hannington et al., 2001; Humphris and Bach, 2005).

Metamorphic rocks, including some of high-pressure origin, also host anhydrite (Nash, 1972; Butchins and Mason, 1973; Liu et al., 2001). Recently, anhydrite has also been found in Martian meteorites (nakhlites), where it is interpreted to record evidence of fluid water at the surface of Mars (Bridges and Grady, 1999; Treiman, 2005; Leshin and Vicenzi, 2006).

Early Observations of Anhydrite in Volcanic Rocks

Two very different occurrences of anhydrite have been described in volcanic rocks. First, and most commonly reported, are anhydrite-bearing xenoliths accidentally incorporated in volcanic deposits. These most likely represent hydrothermally precipitated anhydrite in altered or metasomatized subvolcanic rocks that were carried to the surface as xenoliths by volcanic

eruptions. Disaggregation of these anhydrite-bearing xenoliths can strew anhydrite and associated minerals into the magma during entrainment, complicating interpretations about a primary or xenocrystic origin. Second are truly primary igneous anhydrite crystals precipitated from the silicate melt. Many of the examples discussed in this paper are complicated by the mixing of these two fundamentally different types of anhydrite, and by the rapid, post-eruption dissolution of anhydrite from high-porosity pyroclastic rocks in contact with surfacewaters and groundwaters.

Anhydrite-Bearing Xenoliths Entrained in Volcanic Rocks

The earliest report of anhydrite-bearing xenoliths in volcanic deposits may be that of Lacroix (1893) for Santorini (Greece); later study of a Santorini anhydrite-bearing xenolith by Nicholls (1971) concluded that they formed through metasomatism of basement marbles. Yoshiki (1933) and Kôzu (1934) discussed anhydrite-bearing xenoliths encountered in products from the 1929 Komagatake eruption (Japan). Three different types of xenoliths were described and termed "pyroxene dacite, micronorite, and diabase." In each case the anhydrite occurred in veins, associated with magnetite (pyroxene dacite), pyrrhotite, cordierite, and gypsum (micronorite), or pyrrhotite, anorthite, and hypersthene (diabase). Petrographic sketches of these three occurrences from Kôzu (1934) are shown in Fig. 1. Other examples of anhydrite-bearing xenoliths in volcanic rocks were reported by Taylor (1958) and Arculus et al. (1983) for the 1951 eruption of Mount Lamington (Papua New Guinea), and by Yagi et al. (1972) for the 1970 eruption of Komagatake.

Anhydrite Crystals Reported in Volcanic Rocks Prior to 1982

The first apparent description of possible stable magmatic anhydrite was by Kawano (1948) for a rhyolite from Himeshima (Japan). Taneda (1949) subsequently interpreted the Himeshima anhydrite to have a deuteric origin. The same deuteric interpretation was favored by Katsui (1958) for anhydrite associated with biotite and alkali feldspar in micro-pegmatitic patches in the groundmass of an olivine basalt from Rishiri volcano (Japan). A petrographic sketch of the Rishiri anhydrite from Katsui (1958) is shown in Fig. 2. Dr. Katsui kindly gave me a slice of the Rishiri olivine basalt in 1982, but no anhydrite was found in a thin section prepared without using water.

Taylor (1958) described small irregular crystals of anhydrite in both the 1951 volcanic rocks at Lamington and in older lavas from the southern crater wall. He considered these to be xenocrysts derived from anhydrite-bearing hornblendite xenoliths, which were common in the 1951 products. Importantly, however, Taylor described these xenoliths as "holocrystalline hornblendite containing primary anhydrite." Arculus et al. (1983) reported bulk sulfur isotopic data for two anhydrite-pyrite-bearing lavas from Lamington's southern crater wall with $\delta^{34}S \simeq 0‰$, which they argued to indicate that the anhydrite was of magmatic, rather than sedimentary origin. They suggested two other possible origins for the sulfur in Lamington anhydrites, involving oxidation of xenolithic sulfides or breakdown of xenolithic sulfur-rich scapolite.

The 1982 El Chichón Eruption: Primary Igneous Anhydrite and Excess Gas Release

The 1982 eruption of El Chichón took place between 28 March and 4 April 1982, produced ~2.2 km^3 of trachyandesitic tephra (Carey and Sigurdsson, 1986; equivalent to 1.1 km^3

of dense-rock-equivalent magma at 2.6 g/cm^3) and released 5-9 million tons of SO_2 to the atmosphere (Krueger et al., 1995). Fresh pumices contain plagioclase, hornblende, clinopyroxene, apatite, titanomagnetite, sphene, about 1 vol.% anhydrite, and minor pyrrhotite and other sulfide minerals in a glassy, micro-vesiculated matrix (Luhr et al., 1984). The anhydrite occurs both as isolated crystals in the vesiculated matrix glass (Fig. 3) and as inclusions within silicate phenocrysts (Fig. 4). In both occurrences, anhydrite is commonly associated with apatite, either as crystal clusters across clean interfaces, or as inclusions of apatite in anhydrite. As discussed below, similar associations between these two minerals are characteristic of anhydrite-bearing magmas. These two Ca- and S-bearing minerals appear to have a pronounced tendency for co-nucleation.

I first collected 1982 pumices at El Chichón in mid-April 1982, two weeks after the end of the eruption. I revisited the volcano in February 1983 and recollected pumices after a single rainy season, when ~4 m of rain typically falls. All anhydrite that was not armored as an inclusion in another mineral was already removed from the geological record (Luhr et al., 1984). Rose et al. (1984) studied older rocks exposed in the 1982 crater walls of El Chichón. These older rocks are very similar in composition and mineralogy to the 1982 trachyandesites, with well-preserved anhydrite crystals particularly in the densest, least-vesicular lava samples. Thus, El Chichón appears to have produced similar S-rich trachyandesitic anhydrite-bearing magmas throughout its life. Petrographic evidence for the presence of stable magmatic anhydrite crystals in 1982 El Chichón pumices is one of the greatest legacies of the eruption.

Damon and Montesinos (1978) described the NW-trending Pliocene to Recent volcanic belt in which El Chichón lies as a diffuse transition zone between the Mexican and Central

American Volcanic Arcs, which they named the Chiapanecan Volcanic Arc. They emphasized the intimate relationship in this region between magmatic and metallogenic activity. Among the clasts in the 1982 deposits were a range of non-vesiculated fragments, some representing relatively fresh pre-1982 dome rocks, and others that show overprints on such a protolith of potassic hydrothermal alteration with abundant Mg-rich biotite and veinlets of anhydrite and pyrrhotite (Luhr, 1983) (Fig. 5). As discussed below, these overprints indicate a possible connection between El Chichón magmatism and formation of porphyry-Cu-type magmatic-hydrothermal deposits at depth.

The 1982 El Chichón eruption was also notable for the recognition that the mass of sulfur gases released to the atmosphere (5-9 megatons of SO_2: Krueger et al., 1995) was too large to have been dissolved in the melt phase of the 1.1 km^3 of magma erupted in 1982 at the deduced pre-eruptive magmatic conditions (T = 800-850^oC; P = 2,000 bars; fO_2 = NNO + 1 log unit: Fig. 6). Consequently, Luhr et al. (1984) concluded that a significant fraction of the erupted sulfur was present in a separate gas phase prior to eruption, such that the magma was already vesiculated as it sat prior to eruption at a depth of ~7 km beneath the volcano. This was the first demonstration of "excess gas release" for a volcanic eruption, a concept that is now well established in the volcanological literature.

Experimental Confirmation of Igneous Anhydrite Stability

The discovery of sulfur volcanoes on Jupiter's Moon Io came in 1979, three years before the El Chichón eruption. On this impetus, experimental petrologists began exploring magmatic sulfur under a wide range of conditions. The discovery of primary igneous anhydrite in El

Chichón's 1982 trachyandesitic pumices fed that interest. Carroll and Rutherford (1984) presented the first experimental phase-equilibrium results for primary igneous anhydrite. That pioneering work, and subsequent studies (Carroll and Rutherford, 1985, 1987; Luhr, 1990; Baker and Rutherford, 1996; Rutherford and Devine, 1996; Scaillet et al., 1998; Scaillet and Evans, 1999; Clemente et al., 2004) demonstrated that virtually any silicate melt composition with sufficient sulfur in the system and an oxygen fugacity higher than ~0.5 log units above the synthetic Ni-NiO buffer will precipitate anhydrite. Over a band of fO_2 values, shown in gray on Fig. 6, anhydrite co-exists with a sulfide phase, either pyrrhotite or an immiscible sulfide melt termed intermediate solid solution (Craig and Scott, 1976). Below this range only a sulfide phase is present, and above this range only anhydrite is present (Carroll and Rutherford, 1987).

An important approach in refining this conclusion and for establishing the solubilities of sulfide and sulphate species in silicate melts with changing oxygen fugacity, was the use of the electron microprobe as a mass spectrometer for estimating the $\%S^{6+}$ ($= 100xS^{6+}/(S^{6+}+S^{2-})$) in sulfur-bearing glasses (Fig. 7A). This is accomplished by precisely measuring the sulfur Kα peak position and comparing it to those for pure sulfate and sulfide (Carroll and Rutherford, 1988; Nilsson and Peach, 1993; Wallace and Carmichael, 1994; Metrich and Clocchiatti, 1996; Matthews et al., 1999a; Jugo et al., 2005). These studies permitted definition of the relationship between magmatic oxygen fugacity and the $\%S^{6+}$ in the glass, providing an independent means of assessing magmatic oxygen fugacity (Fig. 7B).

The 1991 Mount Pinatubo Erution: Primary Igneous Anhydrite and Excess Gas Release

Two of the remarkable aspects of the El Chichón eruption, primary igneous anhydrite and

excess gas release, were also noted for the significantly larger Mount Pinatubo eruption just 9 years later. The Pinatubo eruption, judged as one of the world's largest in the 20th century, began its magmatic stages with extrusion on 7 June 1991 of a hybrid andesite dome with quenched basalt inclusions, followed by pre-climactic explosive eruptions of andesite and increasingly abundant dacite. The eruption climax came on 15 June 1991 with a total of 8.4-10.4 km^3 of dacitic pumice and ash (equivalent magma volume of 3.7-5.3 km^3) ejected as about roughly equal amounts of pyroclastic-fall and -flow deposits (Scott et al., 1996). Fresh pumices contained plagioclase, hornblende, titanomagnetite, ilmenite, cummingtonite, biotite, quartz, apatite, anhydrite, sulfides, and rare zircon (Imai et al., 1993; 1996; Bernard et al., 1996; Luhr and Melson, 1996; Pallister et al., 1996). As in the case for El Chichón, the 1991 Pinatubo anhydrite commonly occurs as euhedral to subhedral crystals with clean contacts against vesiculated glass; again clusters and mutual inclusions with apatite crystals are frequently encountered (Bernard et al., 1991 and 1996; Fournelle et al., 1996; Pallister et al., 1996). In Fig. 8 are reproduced three backscattered-electron images from Fournelle et al. (1996) showing such anhydrite-apatite clusters and an anhydrite inclusion hosted by plagioclase, with associated marginal and included apatite. Fournelle et al. (1996) also presented backscattered-electron images of titanomagnetite inclusions within anhydrite, and anhydrite inclusions within hornblende phenocrysts.

The compositions of coexisting Fe-Ti oxides and the presence of cummingtonite in 1991 Mount Pinatubo pumices were used to estimate the pre-eruptive magmatic temperature (T = ~780^{o}C) and oxygen fugacity (fO_2 = NNO + 1.7 log units: Fig. 6) (Evans and Scaillet, 1997). Phase-equilibrium experiments were able to reproduce the observed phase assemblage and

compositions under water-rich (XH_2O_{fluid} >0.88) fluid-saturated pressures of ~2,200 bars, equivalent to a depth of ~9 km (Rutherford and Devine, 1996; Scaillet and Evans, 1999), consistent with the depth of a zone of low seismic velocity beneath the volcano (Mori et al., 1996; Pallister et al., 1996).

One of the most discussed aspects of the 1991 eruption of Mount Pinatubo was its injection into the stratosphere of an estimated 20 million tons of SO_2 (Bluth et al., 1992; Krueger et al., 1995; Guo, et al., 2004), the largest volcanic SO_2 cloud ever measured by modern techniques. This mass of SO_2 is thought to be typical for annual volcanic release to the atmosphere, but represents only about 10% of current total atmospheric SO_2 emissions, which are dominated by human activities (Stoiber et al., 1987; Bluth et al., 1993). An important difference between volcanic and human-based releases of SO_2 is that explosive volcanic eruptions can inject sulfur gases into the stratosphere, above the levels of tropospheric weather and rain. Thus stratospheric SO_2 injections can have long and complex life cycles, and can perturb the Earth's atmospheric temperature structure.

The initial Pinatubo SO_2 gas plume was tracked and sampled by a wide range of ground-, air-, and space-based instruments as it circled the globe and converted to a giant cloud of micron-sized sulfuric acid droplets. The Pinatubo aerosol cloud was considered to have caused global-scale warming of the stratosphere, depletion of stratospheric ozone, and cooling of the atmosphere at the Earth's surface (Halpert et al., 1993; McCormick et al., 1995; Hansen et al., 1996).

Sulfur mass-balance calculations similar to those used by Luhr et al. (1984) to argue for "excess gas release" for the 1982 El Chichón eruption, were also used to support "excess gas

release" for the 1991 Mount Pinatubo eruption (Westrich and Gerlach, 1992; Wallace and Gerlach, 1994; Gerlach et al., 1996). Because the Pinatubo eruption was so much larger in magnitude than the El Chichón eruption, was the second example of the phenomenon, and had measurable global-scale consequences, it cemented the concept of "excess gas release" in the volcanological community, in a way that the first example, the El Chichón eruption, could not. Many other studies have since explored the topic of "excess gas release" at other subduction-zone volcanoes (Andres et al., 1991; Gerlach et al., 1994; Wallace and Anderson, 2000; Wallace, 2001). Sharma et al. (2004) drew attention to the presence of "excess gas release" at subduction-zone volcanoes, and its absence at basaltic volcanoes from oceanic spreading ridges (Iceland) and oceanic hot spots (Hawaii). Critical to the notion of "excess gas release" is the fluid/melt partition coefficient for sulfur. This subject has been explored experimentally by Scaillet and Clemente (1998) and Keppler (1999). They have shown that for oxidized subduction-related magmas of the type erupted at El Chichón in 1982 and Mount Pinatubo in 1991, the fluid/melt partition coefficient is well above 1, strongly favoring sulfur partitioning into H_2O-dominant vapor bubbles relative to the coexisting silicate melt in the pre-eruptive, vesiculating magma reservoir. Jakubowski et al. (2002) presented evidence that in addition to anhydrite precipitating from the Pinatubo melt, anhydrite was also precipitating from magmatic vapor onto mineral surfaces at depth prior to eruption.

Prior to the 1982 eruption of El Chichón, there was little mention in the scientific literature about magmas that were vapor-saturated prior to eruption. Presently, "excess gas release" and the concept of vapor-saturated magmas at depth in the Earth is well established. This is another of the important legacies of the 1982 El Chichón eruption.

Other Examples of Primary Igneous Anhydrite Recognized Since 1982

Many other examples of primary igneous anhydrite (besides 1991 Mount Pinatubo) have been proposed or considered since the 1982 El Chichón eruption. In this section these examples are discussed from youngest to oldest, with volcanic types followed by plutonic types. Representative major-element analyses are listed in Table 1, and a summary of common minerals is listed in Table 2.

Volcanic Examples:

2001-2004 Shiveluch (Russia): Dirksen et al. (2006) investigated the 2001-2004 dome-forming eruption of Shiveluch, which produced a total of 0.27 km^3 of andesitic magma. The dominant phenocrysts are plagioclase, hornblende, orthopyroxene, and titanomagnetite. The groundmass includes the same minerals (excluding hornblende) plus clinopyroxene, ilmenite, cassiterite, sphene, bornite, cuprite, apatite, anhydrite, and glass. Sparse olivine, clinopyroxene, and orthopyroxene xenocrysts with well-developed reaction rims are also present. The pre-eruptive temperature was estimated at ~850^oC based on Fe-Ti-oxide and plagioclase-amphibole geothermometers. The maximum water content measured in glass inclusions was 5.1 wt.% H_2O.

1985 Nevado del Ruiz (Colombia): This deadly eruption produced only about 0.03 km^3 of tephra (Calvache et al., 1987), but an estimated 3.4 x 10^6 g of SO_2 (Williams et al., 1990), an amount far in excess of the sulfur that could have been dissolved in the erupted magma. Thus the 1985 Nevado del Ruiz eruption is another example of "excess gas release." Two different forms of

rare anhydrite were described. One pumice contained irregular aggregates of xenocrystic anhydrite mentioned by Melson et al. (1990) and described in considerable detail by Fournelle (1990). More interesting with regard to potential primary igneous anhydrite, Fournelle (1990) also described a single 25-μm inclusion of anhydrite touching other small inclusions of titanomagnetite and clinopyroxene, all hosted by an orthopyroxene phenocryst in a 1985 pumice. Fournelle (1990) did not favor a primary igneous origin for this anhydrite inclusion.

Lascar (Chile): The late-Pleistocene Piedras Grandes unit is an andesitic dome complex with block-and-ash flow and flood deposits that developed just prior to the 26.5 ka compositionally zoned (dacite to basaltic andesite) major explosive Soncor eruption of 8 km^3 magma. The Piedras Grandes magma was dominantly hornblende andesite, with streaks of basaltic andesite. The Piedras Grandes mineral assemblage consists of plagioclase, hornblende, orthopyroxene, clinopyroxene, titanomagnetite, ferrian-ilmenite, olivine, biotite, quartz, and apatite. Rare anhydrite, pyrrhotite, and zircon are also present, but only as inclusions in titanomagnetite. Coexisting Fe-Ti oxides were used to estimate a temperature of ~915^oC and an oxygen fugacity of NNO + 1.6 log units (Matthews et al., 1999b: Fig. 6).

Sutter Buttes (USA): This Pleistocene (1.36-1.59 Ma) volcanic dome and pyroclastic complex erupted in the northern part of California's Central Valley, at the southern end of the Cascade Range (Williams and Curtis, 1977; Hausback and Nilsen, 1999). A drill core into hornblende andesite on the S side of the complex was added to the University of California, Berkeley, teaching collections in 1949, and was used for many years in the introductory geology

laboratories as an example of the rock type andesite: UCB-103-14. In mid-1982, when I gave an informal lecture to the Berkeley Geology and Geophysics Department about El Chichón's 1982 eruption and the discovery of primary igneous anhydrite, Professor Richard Hay asked me to come to his office to look at a mineral in thin section from that Sutter Buttes drill core sample that had long bothered him. He had thought it was barite. Electron-microprobe analysis confirmed that it was anhydrite. The situation is somewhat complicated by the fact that anhydrite is heterogeneously distributed in the various pieces of the core and that secondary calcite and associated secondary (hydrothermal) anhydrite are present in many core pieces. Nonetheless, intimate intergrowths of igneous apatite and anhydrite demonstrate that at least some of the anhydrite is primary (Fig. 9). The mineral assemblage of sample UCB-103-14 is plagioclase, hornblende, biotite, apatite, titanomagnetite, and anhydrite; a single sphene crystal was observed. The first 5 minerals constitute the typical mineralogy of samples studied from surface exposures at Sutter Buttes (Williams and Curtis, 1977; Hausback and Nilsen, 1999), but those authors have never observed anhydrite or sphene in Sutter Buttes rocks, even as inclusions in other minerals.

These observations point to the ephemeral nature of primary igneous anhydrite in rocks exposed to Earth's hydrosphere, and complications that can ensue when rocks with primary igneous anhydrite survive leaching by the hydrosphere, but are subjected to hydrothermal alteration. A subset of the UCB-104-14 drillcore samples was donated to the Smithsonian collections as NMNH# 116608.

Cerro Lanza (Mexico): I have investigated 15 volcanic rocks (unpublished data) from the

Chiapanecan Volcanic Arc, in which El Chichón lies (Damon and Montesinos, 1978), five of which have nearly identical bulk rock compositions and mineralogy as the 1982 El Chichón trachyandesite. These include the outcrops for sample numbers 7, 9, and 10 from Damon and Montesinos (1978). One of those localities, the eroded lava dome of Cerro Lanza (16.455°N, 92.586°W), lies about 124 km SE of El Chichón, and ~2.5 NNE of the town Nicolás Ruiz (sample 9: Damon and Montesinos, 1978), and rises >100 m above the surrounding landscape (Fig. 10). The only significant mineralogical differences with respect to the 1982 El Chichón trachyandesite, are that the Cerro Lanza trachyandesites have considerably more sphene, but no biotite or anhydrite microphenocrysts. However, a single small inclusion of anhydrite was found armored as an inclusion within a plagioclase phenocryst (Fig. 11), evidence that the Cerro Lanza magma was probably also anhydrite-bearing upon eruption.

Julcani (Peru): High-K rhyodacites and rhyolites of the late-Miocene (9.7-10.2 Ma) Bulolo dike, associated with the Julcani precious-metal mineralization (Ag-Cu-Bi-Pb-Au-W), contain plagioclase (An_{38-57}), hornblende, quartz, and biotite, with lesser apatite, sphene, Fe-Ti oxides, augite, hypersthene, pyrrhotite, and magmatic anhydrite (Drexler and Munoz, 1985; Deen et al., 1994). These observations were made on outcrop samples, not drillcore (John Drexler, personal communication 2006). Drexler and Munoz (1985) used coexisting Fe-Ti oxides to estimate a pre-emplacement temperature for the Bulolo magma of ~840°C and a high oxygen fugacity several log units above the NNO buffer (Fig. 6).

Eagle Mountain (USA): An Oligocene andesite dike erupted at the Eagle Mountain volcanic

center of the San Juan Volcanic Field (Colorado) contains the mineral assemblage plagioclase, hornblende, titanomagnetite, augite, orthopyroxene, S-rich apatite, anhydrite, ilmenite, pyrrhotite, and pyrite. Anhydrite is present only as inclusions within hornblende, whereas globular pyrrhotite grains are included in many other minerals. Coexisting Fe-Ti oxides were used to estimate a temperature of ~890^{o}C and an oxygen fugacity of NNO + 1.3 log units (Fig. 6).

Plutonic Examples:

El Teniente "Porphyry A" (Central Chile): Drillcore samples reveal that this late-Miocene (5.7 Ma) pluton, associated with the world's largest porphyry-Cu deposit, has very abundant anhydrite (to >30 vol.%) with planar crystal boundaries against other silicate minerals, as well as inclusions of the same silicate minerals within anhydrite. Plagioclase is very sodic, and no hornblende is present, although biotite is abundant (up to >50 vol.%), indicating that early anhydrite precipitation locked up most of the calcium in the magma (Funk et al., 2005; Stern et al., 2006).

Santa Rita (USA): Sample SR 8 from a Paleocene (63 Ma) quartz-monzodioritic dike associated with the important producing porphyry-Cu deposit at Santa Rita (New Mexico) (Audétat and Pettke, 2006), contains the mineral assemblage plagioclase, hornblende, biotite, quartz, anhydrite, apatite, sphene, and titanomagnetite. Anhydrite is preserved as inclusions in apatite and sphene, but its former presence as ~1-2 vol.% phenocrysts is inferred from lath-shaped cavities now filled by orange-brown microcrystalline quartz. The mineral assemblage was used

to constrain magmatic oxygen fugacity to >NNO + 1 (Audétat et al., 2004). Sample SR 15 from a rhyodacite porphyry at Santa Rita preserved anhydrite inclusions within plagioclase, hornblende, and apatite crystals. Lath-shaped cavities (1-3 vol.%) now filled with calcite were interpreted as original primary anhydrite crystals (Audétat and Pettke, 2006).

Cajon Pass Deep Drillhole (USA): This deep continental drilling project in southern California encountered more than 1 km of late-Cretaceous (?) intermediate plutonic rocks with primary anhydrite as both isolated phenocrysts and microphenocrysts in poikilitic hornblende, plagioclase, and sphene (Barth and Dorais, 2000). The crystallization conditions were estimated as T = 706°C, P = 6 kb, and oxygen fugacity = NNO + 2 log units.

Yerington (USA): The Yerington batholith in western Nevada is Jurassic in age (~169 Ma) and consists of multiple plutons of quartz monzonite to granite composition associated with porphyry-Cu and copper-iron skarn deposits that contain a total of ~6 million tons of Cu (Dilles, 1987). The plutonic rocks record hydrous and oxidizing conditions. Typical mineral assemblages are plagioclase, microcline, quartz, hornblende, ± augite, biotite, titanomagnetite, ilmenite, sphene, apatite, and zircon (Dilles, 1987). Apatite is present both as inclusions in all major minerals and along their grain boundaries, indicating that it precipitated throughout the crystallization sequence. Apatite crystals commonly show pronounced declines in SO_2 contents from cores to rims, which Streck and Dilles (1998) interpreted to reflect mid- to late-stage "cryptic anhydrite crystallization" that depleted the Yerington melts in sulfur. However, no igneous anhydrite was observed in Yerington rocks not even as inclusions in other minerals

(Streck and Dilles, 1998).

Common Characteristics of High-fO_2 Anhydrite-Bearing Magmas

Hornblende and biotite phenocrysts were shown by Carmichael (1967; 1991) to be characteristic of magmas with oxygen fugacities greater than NNO + 1 log unit. As seen in Table 2, hornblende is present in all but 1 of the 12 anhydrite-bearing volcanic and plutonic examples listed; the exception is El Teniente, where abundant early formed anhydrite sequestered so much CaO that plagioclase is very albitic and Ca-bearing mafic silicates are absent. Biotite, however, is very abundant at El Teniente, and present in 7 of the other 11 examples.

As oxygen fugacity increases in magmatic systems, the Fe^{3+}/Fe^{2+} ratio in the melt also increases, leaving progressively less Fe^{2+} able to compete with Mg^{2+} for site occupancy in mafic minerals. Accordingly, as fO_2 increases, so does the Mg# of mafic minerals (Dilles, 1987; Scaillet and Evans, 1999). Although the latter authors noted that these trends are complicated by the presence of sulfate, high Mg# in mafic minerals appears to be characteristic of high-fO_2 magmas.

Apatite is ubiquitous in anhydrite-bearing rocks (unreported for the Cajon Pass example), and as discussed above, shows a preference for co-nucleation with anhydrite such that intergrowths and mutual inclusions of these two Ca- and S-bearing non-silicate minerals are common in many of the 12 examples listed (Figs. 3, 4, 8, and 9).

Many authors have discussed the significance of sphene as an indicator of high magmatic oxygen fugacity (Verhoogen, 1962; Carmichael and Nicholls, 1967; Lipman, 1971). Wones

(1989) presented an expression for the T-fO_2 dependence of the reaction hedenbergite + ilmenite + O_2 = sphene + magnetite + quartz, which he considered as a proxy for the transition from lower fO_2 ilmenite-bearing magmas to higher fO_2 sphene-bearing magmas. The fO_2 of this reaction lies at NNO for a temperature of ~780°C, and rises to NNO + 1 log unit at ~975°C (Fig. 6). Wones (1989) noted that the reduction of hedenbergite activity in clinopyroxene (or amphibole) below 1 for natural Mg-bearing magmatic systems would shift the reaction curve to higher fO_2. Sphene is present in 8 of the 12 examples of anhydrite-bearing rocks listed in Table 2.

Another common characteristic of many cases of igneous anhydrite is an association with porphyry-copper and other ore deposits (Julcani, Eagle Mountain, El Teniente, Santa Rita, and Yerington); importantly anhydrite is also known as an important mineral in magmatic-hydrothermal ore deposits (Rye, 2005). Furthermore, hornblende and biotite phenocrysts are characteristic of the intermediate-to-felsic plutonic rocks that typically host porphyry-Cu deposits (Lowell, 1974; Gustafson and Hunt, 1975; Audétat et al., 2004). Lithic fragments with potassic-alteration assemblages from the 1982 El Chichón tephra deposit (Luhr, 1983) hint that a porphyry-Cu-type magmatic-hydrothermal ore deposit may be actively forming at depth. Imai et al. (1993; 1996) discussed the close spatial and genetic association between the dacites of Mount Pinatubo and a chain of late-Miocene to Pliocene porphyry-Cu (-gold) deposits that extends through northern and west-central Luzon, including the Dizon deposit ~20 km south of Pinatubo.

Sulfur Isotopes of Anhydrite and Sulfides at El Chichón and Mount Pinatubo

Published measurements of $\delta^{34}S$ in products from the 1982 El Chichón and 1991 Mount

Pinatubo eruptions, by conventional techniques and by secondary-ion mass spectrometry, are discussed in order of their publication and plotted on histograms in Fig. 12.

El Chichón: Conventional Methodology

Sulfur isotopic compositions were reported for bulk separates of anhydrite and sulfides from the 1982 El Chichón pumices and hydrothermally altered lithic fragments (Rye et al., 1984). Anhydrite separates from 3 different pumices had very similar $\delta^{34}S$ values of +9.0, +9.1, and +9.2 ‰, whereas two sulfide separates yielded $\delta^{34}S$ values of +2.7 and +3.6 ‰ (Fig. 12D). This difference between the bulk anhydrite and sulfide separates was found to be consistent with magmatic temperatures in the range 800-850^{o}C, supported by independent analytical and experimental methods (Luhr et al., 1984; Rye et al., 1984). Thus, the anhydrite and pyrrhotite-dominated sulfide assemblage were interpreted to be in isotopic equilibrium in the 1982 magma. Furthermore, the anhydrite was found to be in oxygen isotopic equilibrium with bulk plagioclase and titanomagnetite separates in the same magmatic temperature range (Rye et al., 1984).

Mount Pinatubo: Conventional Methodology

Three different articles in the 1996 Fire and Mud volume discussed conventional sulfur isotopic data for products from the 1991 eruption of Mount Pinatubo (Fig. 12A and B). Bernard et al. (1996) reported $\delta^{34}S$ values for 4 whole-rock samples, 6 soluble-sulfate analyses from whole-rock samples, 2 soluble-sulfate analyses for fresh ash-fall samples, and 1 insoluble-sulfur analysis for a whole-rock sample. The range of $\delta^{34}S$ values for the 15 June dacite is large, even

when only whole-rock data are considered (+6.9 to +12.2 ‰). Soluble-sulfate analyses for two S-rich fresh ash samples collected on 4 July 1991 (+9.4, +9.7 ‰) also fall within this range. A single measurement for soluble sulfate from the 12 June 1991 andesite is slightly lighter than all others (+6.3 ‰). Fournelle et al. (1996) reported a single $\delta^{34}S$ value of +8.2 ‰ for soluble sulfate from a 15 June pumice, and $\delta^{34}S$ values of about +1.0 ‰ for monosulfide and disulfide minerals from the Zambales Ophiolite, which underlies Mount Pinatubo. Imai et al. (1993; 1996) reported six $\delta^{34}S$ values of +7.8‰ to +9.0‰ for HCl-leached sulfate from 15 June pumices (Fig. 12).

Mount Pinatubo: Secondary-Ion Mass Spectrometry

In the same Fire and Mud volume, McKibben et al. (1996) reported sulfur isotopic compositions of Pinatubo anhydrites and sulfides determined by secondary-ion mass spectrometry (SIMS) using the SHRIMP ion-probe at the Australian National University. The 2σ analytical precision of the measurements was 2‰. Fig. 12A-C show those $\delta^{34}S$ values in histograms. For the vent-clearing 12 June andesitic phase of the eruption, individual anhydrite crystals were isotopically homogeneous, but crystal-to-crystal variations in $\delta^{34}S$ were huge, from +3‰ to +16‰ (Fig. 12A). For the paroxysmal 15 June dacite, the observed range was smaller, but still well beyond the 2σ analytical precision (Fig. 12B). Hydrothermal anhydrite and sulfide minerals in Pinatubo drillcore samples showed distinct and homogeneous populations (Fig. 12C).

El Chichón: Secondary-Ion Mass Spectrometry

Inspired by the SIMS study of McKibben and colleagues, Luhr and Logan (2002)

measured sulfur isotopic compositions in anhydrite, primary pyrrhotite, and other sulfides interpreted to be xenocrystic from 1982 El Chichón pumices using the Carnegie Institution ion-probe (Fig. 12D). The 2σ analytical precision of the measurements was 1‰, half that of the McKibben study, reflecting 6 years of progress in analytical-technique development. We found virtually identical results to those of McKibben et al. (1996). Individual anhydrite crystals were isotopically homogeneous, but crystal-to-crystal variations in $\delta^{34}S$ were large (+2.5‰ to +10.9‰). Variations in $\delta^{34}S$ showed no relationship to complex textures revealed by cathodoluminescence color. Two anhydrite crystals sitting side by side surrounded by vesiculated matrix glass (Luhr and Logan, 2002: Fig. 2) were used to illustrate the situation; two spots on crystal 1 yielded $\delta^{34}S$ values of +2.5 and +3.0‰, whereas four spots on crystal 2 ranged from +6.5 to +8.0‰; the difference between these two crystals lies significantly beyond the 2σ analytical precision. Luhr and Logan (2002) also measured sulfur isotopic compositions of 6 ovoid-shaped magmatic sulfide inclusions (pyrrhotite, chalcopyrite, or intermediate sulfide solid solution) in silicate and oxide minerals ($\delta^{34}S$ = -0.1 to +2.7‰; mean 0.7‰), and of 4 irregularly shaped multi-sulfide fragments in the groundmass, interpreted as xenocrystic, which range widely ($\delta^{34}S$ = -3.7‰ to +5.5‰).

Interpretations of Sulfur Isotopic Data

Two different hypotheses have been put forward to explain the similar SIMS results for $\delta^{34}S$ in anhydrites from the 1991 Mount Pinatubo and 1982 El Chichón pumices. McKibben et al. (1996) argued that the Pinatubo isotopic heterogeneity reflects physical mixing of igneous anhydrite with isotopically heavy xenocrystic hydrothermal anhydrite (Fig. 12C). In contrast,

Rye (2005) argued that El Chichón and Pinatubo isotopic heterogeneity reflects quenching of the dynamic, non-equilibrium processes of degassing and crystallization in different magma domains, followed by eruptive mixing of those domains. Future studies are needed to resolve these and other possible explanations. A reliable method of distinguishing magmatic anhydrite from hydrothermal anhydrite that does not rely on the use of sulfur isotopes would be most helpful in this regard.

Conclusions

Primary igneous anhydrites in pumices from both El Chichón in 1982 and Mount Pinatubo in 1991 precipitated from water-rich and oxidized magmas that are thought to have been gas-saturated at 7-9 km depth prior to eruption, where a significant mass of gas existed in H_2O-dominated vapor bubbles. In both cases this interpretation of "excess gas release" was based on analysis of the magmatic sulfur budget. Both eruptions injected large masses of SO_2 gas into the stratosphere, where it quickly converted to form giant clouds of micron-sized sulfuric-acid aerosol droplets capable of affecting the Earth's thermal balance.

Evidence for primary igneous anhydrite has also been confirmed or inferred in at least 10 other localities. Anhydrite is highly soluble in water near Earth's surface, so the survival potential for primary igneous anhydrite is low. In five of the occurrences considered in this study, anhydrite is only present as inclusions within silicate phenocrysts, titanomagnetite, or apatite (Nevado del Ruiz, Lascar, Cerro Lanza, Eagle Mountain, Santa Rita). Anhydrite was completely removed from El Chichón pumices collected 1 year after the eruption, in this area of extremely heavy rainfall (>4 m/yr). Aside from pumices collected immediately after eruption at

El Chichón in 1982 and Mount Pinatubo in 1991, and denser lavas exposed in the new 1982 El Chichón crater, the late-Miocene Bulolo dike at Julcani is the only other location where a surficial outcrop has yielded rock specimens with primary anhydrite microphenocrysts. All other known examples of primary igneous anhydrite not armored as inclusions in another mineral come from drill-core samples: Sutter Buttes, El Teniente, and Cajon Pass.

Whether primary igneous anhydrite is observed directly, or inferred from anhydrite inclusions in other phenocrysts or other criteria, all of those samples have certain features in common. All have plagioclase and hornblende as the two most abundant minerals, the latter an indication of high water contents. All show evidence of high oxygen fugacity (>NNO +1) in either whole-rock Fe^{3+}/Fe^{2+}, fO_2 derived from co-existing Fe-Ti oxides, and/or the presence of sphene. Hornblende and biotite phenocrysts, which were argued by Carmichael (1967; 1991) to signify magmatic oxygen fugacities greater than NNO + 1 log unit, are characteristic of the intermediate-to-felsic plutonic rocks that typically host porphyry-Cu deposits. There appears to be a close connection between occurrences of primary igneous anhydrite and associated ore deposits (Julcani, Eagle Mountain, El Teniente, Santa Rita, and Yerington). Both El Chichón and Mount Pinatubo also lie in zones of metallogenesis.

SIMS analyses of sulfur isotopic compositions for anhydrite crystals in both 1991 Mount Pinatubo and 1982 El Chichón pumices revealed that individual crystals are isotopically homogeneous, but intercrystalline variations in $\delta^{34}S$ are large. These variations may reflect either mixing of primary and xenocrystic anhydrite, or syn-eruptive mixing and quenching of magma parcels that underwent different non-equilibrium processes during degassing and crystallization.

Acknowledgments

Peggy Genaro kindly donated samples from the Sutter Buttes drillcore to the Smithsonian collections for this study. Brian Hausback led me on a tour of the Sutter Buttes to collect additional samples and offered important insight on that unusual volcano. John Fournelle and Washington University Press gave permission to reproduce the backscattered-electron images of apatite-anhydrite clusters and inclusions from Mount Pinatubo as Fig. 8. John Drexler and Chuck Stern shared important information about the Julcani and El Teniente localities, respectively. Tim Rose assisted with back-scattered electron images from El Chichón pumices and Sutter Buttes drill core samples. The reviews of Claus Siebe and José Luis Arce are acknowledged.

References

Africano, F., Bernard, A., 2000. Acid alteration in the fumarolic environment of Usu volcano, Hokkaido, Japan. J. Volcanol. Geotherm. Res. 97, 475-495.

Andres, R.J., Rose, W.I., Kyle, P.R., de Silva, S., Francis, P., Gardeweg, M., Moreno Roa, H., 1991. Excessive sulfur dioxide emissions from Chilean volcanoes. J. Volcanol. Geotherm. Res. 46, 323-329.

Arculus, R.J., Johnson, R.W., Chappell, B.W., McKee, C.O., Sakai, H., 1983. Ophiolite-contaminated andesites, trachybasalts, and cognate inclusions of Mount Lamington, Papua New Guinea: Anhydrite-amphibole-bearing lavas and the 1951 cumulodome: J. Volcanol. Geotherm. Res. 18, 215-247.

Audétat, A., Pettke, T., 2006. Evolution of a porphyry-Cu mineralized magma system at Santa Rita, New Mexico (USA). J. Petrol. 47, 2021-2046.

Audétat, A., Pettke, T., Dolejš, D., 2004. Magmatic anhydrite and calcite in the ore-forming quartz-monzodiorite magma at Santa Rita, New Mexico (USA): genetic constraints on porphyry-Cu mineralization. Lithos 72, 147-161.

Baker, L.L., Rutherford, M.J., 1996. Crystallization of anhydrite-bearing magmas. Trans. Roy.

Soc. Edinb., Earth Sci. 87, 243-250.

Barth, A.P., Dorais, M.J., 2000. Magmatic anhydrite in granitic rocks: First occurrence and potential petrologic consequences. Am. Min. 85, 430-435.

Bernard, A., Demaiffe, D., Mattielli, N., Punongbayan, R.S., 1991. Anhydrite-bearing pumices from Mount Pinatubo: Further evidence for the existence of sulfur-rich silicic magmas. Nature 354, 139-140.

Bernard, A., Knittel, U., Weber, B., Weis, D., Albrecht, A., Hattori, K., Klein, J., Oles, D., 1996. Petrology and geochemistry of the 1991 eruption products of Mount Pinatubo. In: Newhall, C.G., Punongbayan, R.S. (Eds.), Fire and Mud: Eruptions and Lahars of Mount Pinatubo, Philippines. Philippine Inst. Volcanol. Seismol., Quezon City, and Univ. Washington Press, Seattle, WA, pp. 767-797.

Bluth, G.J.S., Doiron, S.D., Schnetzler, C.C., Krueger, A.J., Walter, L.S., 1992. Global tracking of the SO_2 clouds from the June, 1991 Mount Pinatubo eruptions. Geophys. Res. Lett. 19, 151-154.

Bluth, G.J.S., Schnetzler, C.C., Krueger, A.J., Walter, L.S., 1993. New constraints on sulfur dioxide emissions from global volcanism. Nature 366, 327-329.

Bohor, B.F., Glass, B.P., 1995. Origin and diagenesis of K/T impact spherules - From Haiti to Wyoming and beyond. Meteoritics 30, 182-198.

Bottrell, S.H., Newton, R.J., 2006. Reconstruction of changes in global sulfur cycling from marine sulfate isotopes. Earth-Sci. Rev. 75, 59-83.

Bridges, J.C., Grady, M.M., 1999. A halite-siderite-anhydrite-chlorapatite assemblage in Nakhla: Mineralogical evidence for evaporites on Mars. Meteoritics Planet. Sci. 34, 407-415.

Butchins, C.S., Mason, R., 1973. Metamorphic anhydrite in a kyanite-bearing schist from Churchill Falls, Labrador. Min. Mag. 39, 488-490.

Calvache, M., Williams, S.N., Young, R.H., 1987. Distribution and volumes of deposits and dynamics of eruptions of Nevado del Ruiz and Cerro Bravo volcanoes, Colombia, over the past 2100 years. EOS, Trans. Am. Geophys. Un. 67, 16, 405.

Carey, S., Sigurdsson, H., 1986. The 1982 eruptions of El Chichón Volcano, Mexico (2): Observations and numerical modelling of tephra-fall distribution. Bull. Volcanol. 48, 127-141.

Carmichael, I.S.E., 1967. The iron-titanium oxides of salic volcanic rocks and their associated ferromagnesian silicates. Contrib. Mineral. Petrol. 14, 36-64.

Carmichael, I.S.E., 1991. The redox state of basic and silicic magmas: a reflection of their source regions? Contrib. Mineral. Petrol. 106, 129-141.

Carmichael, I.S.E., Nicholls, J., 1967. Iron-titanium oxides and oxygen fugacities in volcanic rocks. J. Geophys. Res. 72, 4665-4687.

Carroll, M.R., Rutherford, M. J., 1985. Sulfide and sulfate saturation in hydrous silicate melts. Proc. 15th Lunar Planet. Sci. Conf., J. Geophys. Res. 90, C601-612.

Carroll, M.R., Rutherford, M.J., 1987. The stability of igneous anhydrite: Experimental results and implications for sulfur behavior in the 1982 El Chichón trachyandesite and other evolved magmas. J. Petrol. 28, 781-801.

Carroll, M.R., Rutherford, M.J., 1988. Sulfur speciation in hydrous experimental glasses of varying oxidation states: Results from measured wavelength shifts of sulfur X-rays. Am. Min. 73, 845-849.

Chou, I.-M., 1978. Calibration of oxygen buffers at elevated P and T using the hydrogen fugacity sensor. Am. Mineral. 63, 690-703.

Claypool, G.E., Holser, W.T., Kaplan, I.R., Sakai, H., Zak, I., 1980. The age curves for sulfur and oxygen isotopes in marine sulfate and their interpretation. Chem. Geol. 28, 199-260.

Clemente, B., Scaillet, B., Pichavant, M., 2004. The solubility of sulfur in hydrous rhyolitic melts. J. Petrol. 45, 2171-2196.

Craig, J.R., Scott, S.D., 1976. Sulfide phase equilibria. In: Ribbe, P.H. (Ed.), Sulfide Mineralogy, Reviews in Mineralogy, v. 1, Mineralogical Society of America, Washington, D.C., pp. CS1-110

Damon, P.E., Montesinos, E., 1978. Late Cenozoic magmatism and metallogenesis over an active Benioff zone in Chiapas, Mexico. Ariz. Geol. Soc. Digest XI, 155-168.

Deen, J.A., Rye, R.O., Munoz, J.L., Drexler, J.W., 1994. The magmatic hydrothermal system at Julcani, Peru: Evidence from fluid inclusions and hydrogen and oxygen isotopes. Econ. Geol. 89, 1924-1938.

Dilles, J.H., 1987. Petrology of the Yerington batholith, Nevada: Evidence for evolution of porphyry copper ore fluids. Econ. Geol. 82, 1750-1789.

Dirksen, O., Humphreys, M.C.S., Pletchov, P., Melnik, O., Demyanchuk, Y., Sparks, R.S.J., Mahony, S., 2006. The 2001-2004 dome-forming eruption of Shiveluch volcano, Kamchatka: Observation, petrological investigation, and numerical modelling. J. Volcanol. Geotherm. Res. 155, 201-226.

Drexler, J.W., Munoz, J.L., 1985. Highly oxidized, pyrrhotite-anhydrite-bearing silicic magmas from the Julcani Ag-Cu-Bi-Pb-Au-W District, Peru: physiochemical conditions of a productive magma. Can. Inst. Mining Conf. on Granite-Related Mineral Deposits: Halifax. September 15-17, 1985. Extended Abstr., 87-100.

Evans, B.W., Scaillet, B., 1997. The redox state of Pinatubo dacite and the ilmenite-hematite solvus. Am. Min. 82, 625-629.

Field, C.W., Zhang, L., Dilles, J.H., Rye, R.O., Reed, M.H., 2005. Sulfur and oxygen isotopic record in sulfate and sulfide minerals of early, deep, pre-Main Stage porphyry Cu-Mo and late Main Stage base-metal mineral deposits, Butte district, Montana. Chem. Geol. 215, 61-93.

Fournelle, J., 1990. Anhydrite in Nevado del Ruiz November 1985 pumice: relevance to the sulfur problem. J. Volcanol. Geotherm. Res. 42, 189-201.

Fournelle, J., Carmody, R., Daag, A.S., 1996. Anhydrite-bearing pumices from the June 15, 1991, eruption of Mount Pinatubo: Geochemistry, mineralogy, and petrology. In: Newhall, C.G., Punongbayan, R.S. (Eds.), Fire and Mud: Eruptions and Lahars of Mount Pinatubo, Philippines. Philippine Inst. Volcanol. Seismol., Quezon City, and Univ. Washington Press, Seattle, WA, pp. 845-863.

Funk, J., Stern, C.R., Skewes, A., Arévalo, A., 2005. Plutonic rocks containing primary igneous

anhydrite in the El Teniente Cu deposit, Chile. Geol. Soc. Am., Abstr. Progr. 37-7, 163.

Gerlach, T.M., Westrich, H.R., Casadevall, T.J, Finnegan, D.L., 1994. Vapor saturation and accumulation in magmas of the 1989-1990 eruption of Redoubt Volcano, Alaska. J. Volcanol. Geotherm. Res. 62, 317-337.

Gerlach, T.M., Westrich, H.R., Symonds, R.B., 1996. Pre-eruption vapor in magma of the climactic Mount Pinatubo eruption: Source of the giant stratospheric sulfur dioxide cloud. In: Newhall, C.G., Punongbayan, R.S. (Eds.), Fire and Mud: Eruptions and Lahars of Mount Pinatubo, Philippines. Philippine Inst. Volcanol. Seismol., Quezon City, and Univ. Washington Press, Seattle, WA, pp. 415-433.

Guo, S. Bluth, G.J.S., Rose, W.I., Watson, I.M., and Prata, A.J., 2004. Re-evaluation of SO_2 release of the 15 June 1991 Pinatubo eruption using ultraviolet and infrared satellite sensors. G^3: Geochem., Geophys., Geosyst. 5, 4. doi: 10.1029/2003GC000654.

Gustafson, L.B., Hunt, J.P., 1975. The porphyry copper deposit at El Salvador, Chile. Econ. Geol. 70, 857-912.

Halpert, M.S., Ropelewski, C.F., Karl, T.R., Angell, J.K., Stowe, L.L., Heim, Jr., R.R., Miller, A.J., Rodenhuis, D.R., 1993. 1992 brings return to moderate global temperatures. EOS, Trans. Am. Geophys. Un. 74, 38, 433-439.

Hannington, M., Herzig, P., Stoffers, P., Scholten, J., Botz, R., Garbe-Schonberg, D., Jonasson, I.R., Roest, W., 2001. Shipboard Scientific Party: First observations of high-temperature submarine hydrothermal vents and massive anhydrite deposits off the north coast of Iceland. Mar. Geol. 177, 3-4, 199-220.

Hansen, J., Ruedy, R., Sato, M., 1996. Global surface air temperature in 1995: Return to pre-Pinatubo level. Geophys. Res. Lett. 23, 13, 1665-1668.

Hausback, B.P., Nilsen, T.H., 1999. Sutter Buttes. In: Wagner, D.L., Graham, S.A. (Eds.), Geologic Field Trips in northern California: Centennial Meeting of the Cordilleran Section of the Geological Society of America, Spec. Publ. 119, Calif. Div. Mines Geol., 246-254.

Holser, W.T., 1977. Catastrophic chemical events in the history of the oceans. Nature 267, 403-408.

Huebner, J.S., Sato, M., 1970. The oxygen fugacity-temperature relationships of manganese oxide and nickel oxide buffers. Am. Mineral. 55, 934-952.

Humphris, S.E., Bach, W., 2005. On the Sr isotope and REE compositions of anhydrites from the TAG seafloor hydrothermal system. Geochim. Cosmochim. Acta 69, 6, 1511-1525.

Imai, A., Listanco, E.L., Fujii, T., 1993. Petrologic and sulfur isotopic significance of highly oxidized and sulfur-rich magma of Mt. Pinatubo, Philippines. Geology 21, 699-702.

Imai, A., Listanco, E.L., Fujii, T., 1996. Highly oxidized and sulfur-rich dacitic magma of Mount Pinatubo: Implications for metallogenesis of porphyry copper mineralization in the western Luzon arc. In: Newhall, C.G., Punongbayan, R.S. (Eds.), Fire and Mud: Eruptions and Lahars of Mount Pinatubo, Philippines. Philippine Inst. Volcanol. Seismol., Quezon City, and Univ. Washington Press, Seattle, WA, pp. 865-874.

Izett, G.A., 1991. Tektites in Cretaceous-Tertiary boundary rocks on Haiti and their bearing on the Alvarez impact extinction hypothesis. J. Geophys. Res. Planets 96, E4, 20,879-20,905.

Jakubowski, R.T., Fournelle, J., Welch, S., Swope, R.J., Camus, P., 2002. Evidence for magmatic vapor deposition of anhydrite prior to the 1991 climactic eruption of Mount Pinatubo, Philippines. Am. Min. 87, 1029-1045.

Jugo, P.J., Luth, R.W., Richards, J.P., 2005. Experimental data on the speciation of sulfur as a function of oxygen fugacity in basaltic melts. Geochim. Cosmochim. Acta 69, 497-503.

Katsui, Y., 1958. Groundmass anhydrite in the olivine basalt from the Rishiri volcano, Hokkaido. J. Jap. Assoc. Min., Pet., Econ. Geol. 42, 188-191 (in Japanese).

Keppler, H., 1999. Experimental evidence for the source of excess sulfur in explosive volcanic eruptions. Science 284, 1652-1654.

Kôzu, S., 1934. The great activity of Komagatake in 1929. Miner. Petrogr. Mitt. 45, 133-174.

Kwano, Y., 1948. A new occurrence of phenocrystic anhydrite crystals in the glassy rocks from Himeshima, Oita Prefecture, Japan: Geol. Surv. Jap. Report 126, 1-7.

Krueger, A.J., Walter, L.S., Bhartia, P.K., Schnetzler, C.C., Krotkov, N.A., Sprod, I., Bluth, G.J.S., 1995. Volcanic sulfur dioxide measurements from the total ozone mapping spectrometer instruments. J. Geophys. Res. 100, 14057-14076.

Lacroix, A., 1893. Les enclaves des roches volcaniques. Macon, Protat Freres: 710 pp.

Leshin, L.A., Vicenzi, E., 2006. Aqueous processes recorded by Martian meteorites: Analysing Martian water on Earth. Elements 2, 159-164.

Lipman, P.W., 1971. Iron-titanium oxides phenocrysts in compositionally zoned ash-flow sheets from southern Nevada. J. Geol. 79, 438-456.

Liu, J.B., Ye, K., Maruyama, S.N., Cong, B.L., Fan, H.R., 2001. Mineral inclusions in zircon from gneisses in the ultrahigh-pressure zone of the Dabie Mountains, China. J. Geol. 109, 4,

523-535.

Lowell, J.D., 1974, Regional characteristics of porphyry copper deposits of the southwest. Econ. Geol. 69, 601-617.

Luhr, J.F., 1983. The 1982 eruptions of El Chichón and the relationship to mineralized magmatic-hydrothermal systems. Geol. Soc. Am. Abstr. Prog. 15, 6, 632.

Luhr, J.F., 1990. Experimental phase relations of water- and sulfur-saturated arc magmas and the 1982 eruptions of El Chichón Volcano. J. Petrol. 31, 1071-1114.

Luhr, J.F., Carmichael, I.S.E., Varekamp, J.C., 1984. The 1982 eruptions of El Chichón Volcano, Chiapas, México: Mineralogy and petrology of the anhydrite-bearing pumices. J. Volcanol. Geotherm. Res. 23, 69-108.

Luhr, J.F., Logan, M.A.V., 2002. Sulfur isotope systematics of the 1982 El Chichón trachyandesite: An ion-microprobe study. Geochim. Cosmochim. Acta 66, 3303-3316.

Luhr, J.F., Melson, W.G., 1996. Mineral and glass compositions in June 15, 1991 pumices: evidence for dynamic disequilibrium in the Pinatubo dacite. In: Newhall, C.G., Punongbayan, R.S. (Eds.), Fire and Mud: Eruptions and Lahars of Mount Pinatubo, Philippines. Philippine Inst. Volcanol. Seismol., Quezon City, and Univ. Washington Press, Seattle, WA, pp. 733-750.

Matthews, S.J., Moncrieff, D.H.S., Carroll, M.R., 1999a. Empirical calibration of the sulphur valence oxygen barometer from natural and experimental glasses: Methods and applications. Min. Mag. 63, 3, 421-431.

Matthews, S.J., Sparks, R.S.J., Gardeweg, M.C., 1999b. The Piedras Grandes - Soncor eruptions, Lascar Volcano, Chile; Evolution of a zoned magma chamber in the central Andean upper crust. J. Petrol. 40, 1891-1919.

McCormick, M.P., Thomason, L.W., Trepte, C.R., 1995. Atmospheric effects of the Mt Pinatubo eruption. Nature 373, 399-373.

McKibben, M.A., Eldridge, C.S., Reyes, A.G., 1996. Sulfur isotopic systematics of the June 1991 Mount Pinatubo eruptions: A SHRIMP ion microprobe study. In: Newhall, C.G., Punongbayan, R.S. (Eds.), Fire and Mud: Eruptions and Lahars of Mount Pinatubo, Philippines. Philippine Inst. Volcanol. Seismol., Quezon City, and Univ. Washington Press, Seattle, WA, pp. 825-843.

Melson, W.G., Allan, J.F., Jerez, D.R., Nelen, J., Clavache, M.L., Williams, S.N., Fournelle, J., Perfit, M., 1990. Water contents, temperatures, and diversity of the magmas of the catastrophic eruption of Nevado del Ruiz, Colombia, November 13, 1985. J. Volcanol. Geotherm. Res. 41, 97-126.

Metrich, N., Clocchiatti, R., 1996. Sulfur abundance and its speciation in oxidized alkaline melts. Geochim. Cosmochim. Acta 60, 21, 4151-4160.

Mori, J., Eberhart-Phillips, D., Harlow, D.H., 1996. Three-dimensional velocity structure at Mount Pinatubo: Resolving magma bodies and earthquake hypocenters. In: Newhall, C.G., Punongbayan, R.S. (Eds.), Fire and Mud: Eruptions and Lahars of Mount Pinatubo, Philippines. Philippine Inst. Volcanol. Seismol., Quezon City, and Univ. Washington Press, Seattle, WA, pp. 371-382.

Nash, C.R., 1972. Primary anhydrite in Precambrian gneisses from the Swakopmund District, South West Africa. Contrib. Mineral. Petrol. 36, 27-32.

Nicholls, I.A., 1971. Calcareous inclusions in lavas and agglomerates of Santorini volcano: Contrib. Mineral. Petrol. 30, 261-276.

Nilsson, K., Peach, C.L., 1993. Sulfur speciation, oxidation state, and sulfur concentration in backarc magmas. Geochim. Cosmochim. Acta 57, 3807-3813.

Pallister, J.S., Hoblitt, R.P., Meeker, G.P., Knight, R.J., Siems, D.F., 1996. Magma mixing at Mount Pinatubo: Petrographic and chemical evidence from the 1991 deposits. In: Newhall, C.G., Punongbayan, R.S. (Eds.), Fire and Mud: Eruptions and Lahars of Mount Pinatubo, Philippines. Philippine Inst. Volcanol. Seismol., Quezon City, and Univ. Washington Press, Seattle, WA, pp.

687-731.

Pape, H., Clauser, C., Iffland, J., Krug, R., Wagner, R., 2005. Anhydrite cementation and compaction in geothermal reservoirs: Interaction of pore-space structure with flow, transport, P-T conditions, and chemical reactions. Int. J. Rock Mech. Mining Sci. 42, 7-8, 1056-1069.

Parat, F., Dungan, M.A., Streck, M.J., 2002. Anhydrite, pyrrhotite, and sulfur-rich apatite: tracing the sulfur evolution of an Oligocene andesite (Eagle Mountain, CO, USA). Lithos 64, 63-75.

Rose, W.I., Jr., Bornhorst, T.J., Halsor, S.P., Capaul, W.A., Plumley, P.S., De la Cruz-Reyna, S., Mena, M., Mota, R., 1984. Volcán El Chichón, Mexico: Pre-1982 S-rich eruptive activity. J. Volcanol. Geotherm. Res. 23, 147-167.

Rutherford, M.J., Devine J.D., 1996. Pre-eruption pressure-temperature conditions and volatiles in the 1991 dacitic magma of Mount Pinatubo. In: Newhall, C.G., Punongbayan, R.S. (Eds.), Fire and Mud: Eruptions and Lahars of Mount Pinatubo, Philippines. Philippine Inst. Volcanol. Seismol., Quezon City, and Univ. Washington Press, Seattle, WA, pp. 751-766.

Rye, R.O., 2005. A review of the stable-isotope geochemistry of sulfate minerals in selected igneous environments and related hydrothermal systems. Chem. Geol. 215, 1-4, 5-36.

Rye, R.O., Luhr, J.F., Wasserman, M.D., 1984. Sulfur and oxygen isotope systematics of the 1982 eruptions of El Chichón Volcano, Chiapas, Mexico. J. Volcanol. Geotherm. Res. 23, 109-123.

Sasaki, M., Fujimoto, K., Tsukamoto, H., Sawaki, T., Sasada, M., Kurosawa, M., Yagi, M., Muramatsu, Y., Kato, O., Komatsu, R., Kasai, K., Doi, N., 2003. Geochemical features of vein anhydrite from the Kakkonda geothermal system, northeast Japan. Resource Geol. 53, 2, 127-142.

Scaillet, B., Clemente, B., 1998. Redox control of sulfur degassing in silicic magmas. J. Geophys. Res. 103, 23,937-23,949.

Scaillet, B., Clemente, B., Evans, B.W., Pichavant, M., 1998. Redox control of sulfur degassing in silicic magmas. J. Geophys. Res. 103, 23937-23949.

Scaillet, B., Evans, B.W., 1999. The 15 June 1991 eruption of Mount Pinatubo. I. Phase equilibria and pre-eruption P - T - fO_2 - fH_2O conditions of the dacite magma. J. Petrol. 40, 381-411.

Scott, W.E., Hoblitt, R.P., Torres, R.C., Self, S., Martinez, M.M.L., Nillos, Jr., T., 1996. Pyroclastic flows of the June 15, 1991, climactic eruption of Mount Pinatubo. In: Newhall, C.G., Punongbayan, R.S. (Eds.), Fire and Mud: Eruptions and Lahars of Mount Pinatubo, Philippines.

Philippine Inst. Volcanol. Seismol., Quezon City, and Univ. Washington Press, Seattle, WA, pp. 545-570.

Sharma, K., Blake, S., Self, S., Krueger, A.J., 2004. SO_2 emissions from basaltic eruptions, and the excess sulfur issue. Geophys. Res. Lett. 31, doi:10.1029/2004JB003033.

Shikazono, N., Kusakabe, M., 1999. Mineralogical characteristics and formation mechanism of sulfate-sulfide chimneys from Kuroko area, Mariana Trough and mid-ocean ridges. Resource Geol. Spec. Issue, 20, 1-11.

Spencer, R.J., 2000. Sulfate minerals in evaporite deposits. Rev. Mineral. Geochem. 40, 173-192.

Stern, C.R., Funk, J.A., Skewes, M.A., Arévalo, A., 2006. Plutonic rocks containing primary igneous anhydrite in the El Teniente Cu megabreccia deposit, central Chile. XI Congresso Geológico Chileno, Antofagasta, Actas 2, 355-358.

Stern, C.R., Funk, J.A., Skewes, M.A., 2007. Sulfur- and copper-rich magmas at El Teniente Cu-Mo deposit, Chile: evidence from plutonic rocks containing primary igneous anhydrite. Geology (draft ms)

Stoiber, R.E., Rose, W.I., Jr., 1974. Fumarole incrustations at active Central American

volcanoes. Geochim. Cosmochim. Acta 38, 495-516.

Stoiber, R.E., Williams, S.N., Huebert, B., 1987. Annual contribution of sulfur dioxide to the atmosphere by volcanoes. J. Volcanol. Geotherm. Res. 33, 1-8.

Streck, M.J., Dilles, J.H., 1998. Sulfur evolution of oxidized arc magmas as recorded in apatite from a porphyry copper batholith. Geology 26, 523-526.

Taneda, S., 1949. On the anhydrite from Himeshima lava. J. Jap. Assoc. Min., Pet., Econ. Geol. 33, 69-73.

Taylor, G.A., 1958. The 1951 eruption of Mount Lamington, Papua: Bur. Mineral Res. Geol.Geophys. Bull. 38, 1-117.

Treiman, A.H., 2005. The nakhlite meteorites: Augite-rich igneous rocks from Mars. Chemie der Erde - Geochem. 65, 3, 203-270.

Verhoogen, J., 1962. Distribution of titanium between silicates and oxides in igneous rocks. Am. J. Sci. 260, 211-220.

Wallace, P.J., 2001. Volcanic SO_2 emissions and the abundance and distribution of exsolved gas in magma bodies. J. Volcanol. Geotherm. Res. 108, 85-106.

Wallace, P., Anderson, A.T., Jr., 2000. Volatiles in magmas. In: Sigurdsson, H. et al. (Eds.), Encyclopedia of Volcanoes, Academic Press, pp. 149-170.

Wallace, P., Carmichael, I.S.E., 1994. S speciation in submarine basaltic glasses as determined by measurements of SKα X-ray wavelength shifts. Am. Min. 79, 161-167.

Wallace, P., Gerlach, T.M., 1994. Magmatic vapor source for sulfur dioxide released during volcanic eruptions: Evidence from Mount Pinatubo. Science 265, 497-499.

Warren, J., 1999. Evaporites: their evolution and economics. Oxford, Malden, MA. Blackwell Science, 438 pp.

Westrich, H.R., Gerlach, T.M., 1992. Magmatic gas source for the stratospheric SO_2 cloud from the June 15, 1991 eruption of Mount Pinatubo. Geology 20, 867-870.

Williams, H., Curtis, G.H., 1977. The Sutter Buttes of California: A study of Plio-Pleistocene volcanism. Univ. Calif. Publ. Geol. Sci. 116, pp. 1-56, 6 plates.

Williams, S.N., Sturchio, N.C., Calvache, M.L., Londoño, A., García, N., 1990. Sulfur dioxide from Nevado del Ruiz volcano, Colombia: Total flux and isotopic constraints on its origins. J. Volcanol. Geotherm. Res. 42, 53-68.

Wones, D.R., 1989. Significance of the assemblage titanite + magnetite + quartz in granitic rocks. Am. J. Sci.74, 744-749.

Yagi, K., Takeshita, H., Oba, Y., 1972. Petrological study of the 1970 eruptions of Akita Komagatake Volcano, Japan. J. Fac. Sci., Hokkaido Univ., Japan, Ser. IV, 15, 109-138.

Yang, W.B., Ahrens, T.J., 1998. Shock vaporization of anhydrite and global effects of the K/T bolide. Earth Planet. Sci. Lett. 156, 3-4, 125-140.

Yoshiki, B., 1933. Activity of Akita-Komagatake volcano. J. Jpn. Assoc. Min. Petr. Econ. Geol. 9: 153-160.

Zimbelman, D.R., Rye, R.O., Breit, G.N., 2005. Origin of secondary sulfate minerals on active andesitic stratovolcanoes. Chem. Geol. 215, 37-60.

Figure Captions

Fig. 1 - Anhydrite-bearing xenoliths from the VEI-4 eruption of Komagataké (Japan) in 1929, reproduced from Figs. 13, 14, and 15b in Kôzu (1934) using original terminology: (A) anhydrite (*A*) and magnetite (*Mt*) vein cutting through pyroxene dacite xenolith. Other mineral abbreviations: *Q* = quartz, *L* = labradorite, *Pl* = plagioclase. Diameter of image = 0.5 mm; (B) anhydrite (*A*), cordierite (*C*), and pyrrhotite (*P*) vein in micronoritic xenolith. Other mineral abbreviations: *Gp* = gypsum, *Hy* = hypersthene, *Pl* = plagioclase. Width of image = 2.1 mm; (C) vein of anhydrite (*A*), pyrrhotite (*P*), and poikilitic anorthite (*An*) with inclusions of pyroxene (*Py*). Diameter of image = 0.5 mm

Fig. 2 - Deuteric anhydrite in micropegmatite patches in the Rishiri (Japan) olivine basalt, reproduced from Katsui (1958). Diameter of image = 1 mm. Mineral abbreviations: Pl = plagioclase, Ol = olivine, Au = augite, Bi = biotite, Af = alkali feldspar, Ah = anhydrite, and C = cavity.

Fig. 3 - Backscattered-electron images of isolated anhydrite crystals surrounded by vesiculated glass in 1982 El Chichón pumices: (A) anhydrite (*an*) cluster with apaitite (*ap*) across a clean straight contact, both surrounded by vesiculated glass; anhydrite also has a small inclusion of apatite; (B) anhydrite crystal with small apatite inclusions surrounded by vesiculated glass; the upper left margin of the anhydrite was resorbed prior to eruptive quenching; (C) anhydrite crystal with apatite inclusion surrounded by vesiculated glass; (D) enlargement of upper left

portion of anhydrite crystal in C showing a small euhedral anhydrite surrounded by vesiculated glass (*vg*) and two adjacent apatite crystals.

Fig. 4 - Backscattered-electron images of anhydrite inclusions in hornblende: (A) hornblende (*hb*) phenocryst surrounded by vesiculated glass with rimward inclusions of sphene (*sp*), titanomagnetite (*t*), and anhydrite (*an*); (B) enlargement of the anhydrite inclusion in hornblende from A showing small apatite (*ap*) crystals and patches of vesiculated glass (*vg*) along the host-inclusion interface; the hornblende also shows a glass inclusion (*gi*); (C) euhedral hornblende phenocryst surrounded by vesiculated glass with a chain of anhydrite (*an*) inclusions along its rim; one anhydrite is completely overgrown by hornblende, whereas the others are still in contact with the vesiculated glass; also present in the hornblende are a glass inclusion (*gi*), apatite (*ap*), titanomagnetite (*t*), and many bright spots that are rich in Sr-Na-Se, the largest of which is 16 microns across; (D) enlargement of one cluster of spherical Sr-Na-Se blebs from C.

Fig. 5 - Secondary anhydrite (*an*) and pyrite (*py*) in a hydrothermally altered lithic fragment from the 1982 pumice-fall deposit of El Chichón. Plagioclase (*pl*) crystals are also labeled.

Fig. 6 - T (^{o}C) versus log fO_2 plot showing estimates for 5 anhydrite-bearing igneous rocks discussed in the text: 1982 El Chichón trachyandesite (Luhr, 1984; Rye et al., 1984); 1991 Mount Pinatubo dacite (Evans and Scaillet, 1997); Lascar, Piedres Grandes unit (*Lasc*: Mathews et al., 1999b); Julcani, Bulolo Dike (*Julc*: Drexler and Munoz, 1985); and Eagle Mountain andesite (*EM*: Parat et al., 2002). Four solid curves show the solid-oxygen buffers nickle-

bunsenite (*Ni-NiO*: Huebner and Sato, 1970), fayalite-magnetite-quartz (*FMQ*), manganosite-hausmanite (*Mn-Hsm*), and magnetite-hematite (*Mt-Hm*) from Chou (1978). The gray stippled area is the field for coexisting anhydrite and pyrrhotite, bounded below by the dashed curve marking minimum fO_2 values for anhydrite stability (*Anhy-In*) from Carroll and Rutherford (1987) and above by the dashed curve marking maximum fO_2 values for pyrrhotite stability (*Po-Out*) from Carroll and Rutherford (1987). The dashed curve labeled *Sphene-In* shows the minimum fO_2 values for sphene stability from the Mg-free reaction hedenbergite + ilmenite + O_2 = sphene + magnetite + quartz (Wones, 1989). The dotted lines labeled 10%, 50%, 70%, and 90% indicate the percentage of melt sulfur in the oxidized S^{6+} state after Matthews et al. (1999a).

Fig. 7 - (A) Examples of the sulfur Kα peaks for S^{6+} in anhydrite and for S^{2-} in troilite determined by electron microprobe (PETH crystal), illustrating a peak shift of 0.0973 mm. This peak shift is used to estimate $\%S^{6+}$ (= $100xS^{6+}/(S^{6+}+S^{2-})$) for volcanic glasses based on the peak position determined for the glass. (B) Three different formulations of the relationship between oxygen fugacity (as ΔNNO = log fO_2 in sample - log fO_2 for the Ni-NiO solid oxygen buffer of Huebner and Sato, 1970) and $\%S^{6+}$: Carroll and Rutherford (1988), Wallace and Carmichael (1994), and Matthews et al. (1999a).

Fig. 8 - Backscattered-electron images of white pumice from the 15 June 1991 Mount Pinatubo eruption, reproduced from Fig. 6 of Fournelle et al. (1996). (A) anhydrite (*An*) inclusion in plagioclase (*Pl*) and two clusters of anhydrite and apatite (*Ap*). (B) Close-up of the anhydrite inclusion in plagioclase from (A) showing associated and included apatite. (C) Close-up of the

farthest right apatite-anhydrite cluster from (A).

Fig. 9 - (A) Plain-light photomicrograph from Sutter Buttes drill-core sample UCB-103-14 (NMNH# 116608) shows a cluster of anhydrite (*an*) and apaitite (*ap*) across a clean straight contact and a nearby hornblende (*hb*) phenocryst. Image is 0.75 mm across. (B) Backscattered-electron image of the same anhydrite-apatite cluster.

Fig. 10 - Photo of Cerro Lanza from 2.5 km away to the SSW in the town of Nicolás Ruiz. Cerro Lanza rises >100 m above the surrounding landscape.

Fig. 11 - (A) Photomicrograph of anhydrite inclusion (40 μm x 15 μm) in plagioclase phenocryst from Cerro Lanza in cross-polarized light. (B) Broader view of host plagioclase phenocryst in crossed-polarized light. Rectangle shows the area of A.

Fig. 12 - Histograms of ion-microprobe $\delta^{34}S$ values for anhydrites and sulfide minerals from 1991 Mount Pinatubo pumices (A, B: McKibben et al., 1996) and hydrothermal samples (C: McKibben et al., 1996) and 1982 El Chichón pumices (D: Luhr and Logan, 2002). Symbols above the historgram peaks show conventional $\delta^{34}S$ values for whole-rock samples, soluble-sulfate analyses for whole-rock samples, soluble-sulfate analyses for fresh ash-fall samples (A & B: Bernard et al., 1996; Imai et al., 1996; and Fournelle et al., 1996), and mineral separates from pumices (D: Rye et al., 1984). Those upper symbols for conventional $\delta^{34}S$ measurements are shown schematically using solid dots for sulfate and solid squares for sulfide. In B, the range for

16 different data is shown.

Table 1. Representative major-element analyses of anhydrite-bearing rocks discussed in this study.

Type:	**Volcanic**	**Volcanic**	**Volcanic**	**Volcanic**	**Volcanic**	**Volcanic**	**Volcanic**	**Plutonic**	**Plutonic**
Volcano:	**El Chichon**	**Pinatubo**	**Shiveluch**	**Lascar**	**S. Buttes**	**Julcani**	**Eagle Mtn.**	**El Teniente**	**Santa Rita**
Sample:	**CH-70-BW**	**White**	**SHV202003**	**GLA-101**	**UCB-103-14**	**4M**	**1**	**970 m**	**SR8**
Year/Age:	**1982**	**1991**	**2002**	**26.5 ka**	**~1.4 Ma**	**~10 Ma**	**~28 Ma**	**5.7 Ma**	**63 Ma**
(wt.%)									
SiO_2	55.88	64.19	61.54	60.07	62.24	67.68	61.55	48.45	63.40
TiO_2	0.71	0.50	0.57	0.65	0.50	0.54	0.74	1.01	0.50
Al_2O_3	17.80	16.69	16.61	16.74	17.29	14.34	16.70	18.62	16.10
Fe_2O_3	2.59	1.93		3.69	1.99		4.62	7.54	
FeO	3.42	2.18	4.67	2.66	2.84	2.95	1.80		4.40
MnO	0.19	0.10	0.09	0.07	0.09	0.06	0.08	0.03	0.05
MgO	2.18	2.39	3.60	3.32	4.54	1.30	1.99	4.73	2.00
CaO	7.91	5.13	5.85	5.36	6.15	2.47	5.30	5.73	5.10
Na_2O	4.46	4.42	4.97	3.61	4.18	3.87	3.98	4.33	2.50
K_2O	2.80	1.51	1.21	2.16	2.24	3.77	2.53	3.63	2.50
P_2O_5	0.43	0.19	0.16	0.19	0.23	0.17	0.34	0.22	
SO_3^{tot}	1.24	0.17				0.28	0.05	1.44	
LOI	0.10	0.60	0.27	1.00	-2.56			4.66	
Total	99.71	100.00	99.54	99.52	99.73	97.43	99.68	100.39	96.55
Normalized with all Fe as FeO and without SO_3 and LOI (wt.%)									
SiO_2	56.96	64.81	61.99	61.20	60.97	69.67	62.07	51.80	65.67
TiO_2	0.72	0.50	0.57	0.66	0.49	0.56	0.75	1.08	0.52
Al_2O_3	18.14	16.85	16.73	17.06	16.94	14.76	16.84	19.91	16.68
FeO^{tot}	5.86	3.95	4.70	6.09	4.54	3.04	6.01	7.25	4.56
MnO	0.19	0.10	0.09	0.07	0.09	0.06	0.08	0.03	0.05
MgO	2.22	2.41	3.63	3.38	4.45	1.34	2.01	5.06	2.07
CaO	8.06	5.18	5.89	5.46	6.02	2.54	5.34	6.13	5.28
Na_2O	4.55	4.46	5.01	3.68	4.09	3.98	4.01	4.63	2.59
K_2O	2.85	1.52	1.22	2.20	2.19	3.88	2.55	3.88	2.59
P_2O_5	0.44	0.19	0.16	0.19	0.23	0.17	0.34	0.24	0.00
Total	100.00	100.00	100.00	100.00	100.00	100.00	100.00	100.00	100.00

Data sources - El Chichón: Luhr et al. (1984); Pinatubo: Luhr and Melson (1996); Shiveluch: Dirksen et al. (2006); Lascar: Matthews et al. (1999); Sutter Buttes: this study; Julcani: Drexler and Munoz (1985); Eagle Mountain: Parat et al. (2002); El Teniente: Stern et al. (2007); Santa Rita: Audétat and Pettke (2006) - the published MnO value of 0.50 wt.% is assumed to actually be 0.05 wt.%.

Table 2. Summary of common minerals in the anhydrite-bearing rocks discussed in this study.

Locality	Anhydrite*	Hornblende	Biotite	Apatite	Sphene	Rock Type
Volcanic						
El Chichón	Yes: mp	Yes	Yes	Yes	Yes	Trachyandesite
Pinatubo	Yes: mp	Yes	Yes	Yes	No	Dacite
Shiveluch	Yes: gm	Yes	No	Yes	Yes	Andesite
Lascar	Yes: incl	Yes	Rare	Yes	No	Andesite to Dacite
Sutter Buttes	Yes: mp	Yes	Yes	Yes	Yes**	Andesite
Cerro Lanza	Yes: incl	Yes	No	Yes	Yes	Trachyandesite
Julcani	Yes: mp	Yes	Yes	Yes	Yes	Dacite to Rhyolite
Eagle Mountain	Yes: incl	Yes	No	Yes	No	Andesite
Plutonic						
El Teniente	Yes: mp	No	Yes	Yes	No	"Microdiorite"
Santa Rita	Yes: incl	Yes	Yes	Yes	Yes	Quartz-Monzodiorite
Cajon Pass	Yes: ph	Yes	Yes	??	Yes	Tonalite to Granodiorite
Yerington	Inferred	Yes	Yes	Yes	Yes	Quartz-Monzodiorite to Granite

*Anhydrite: ph = phenocryst (>0.3 mm across); mp = anhydrite microphenocryst (<0.3 mm & >0.03 mm across); incl = anhydrite inclusion in silicate or oxide mineral; gm assumed to mean <0.03 mm across, but not specified in the source publication.
** one crystal was observed in one section of UCB-103-14. No other sphene has been reported for Sutter Buttes.

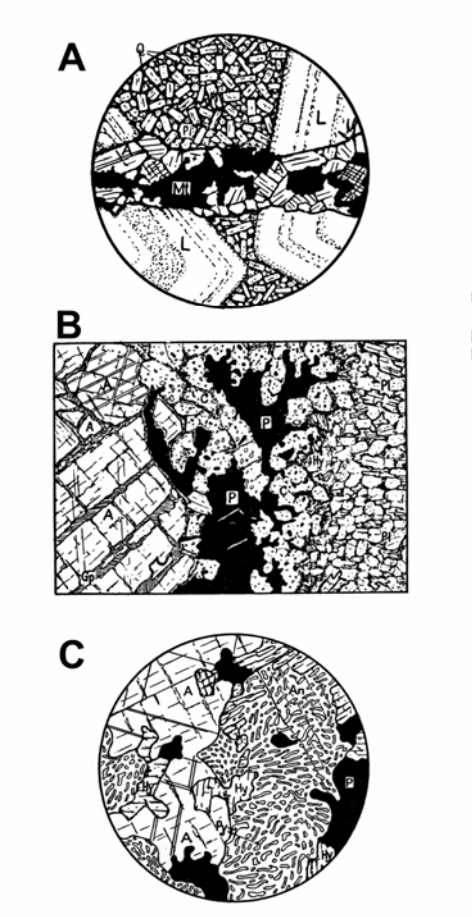

Luhr – Fig. 1

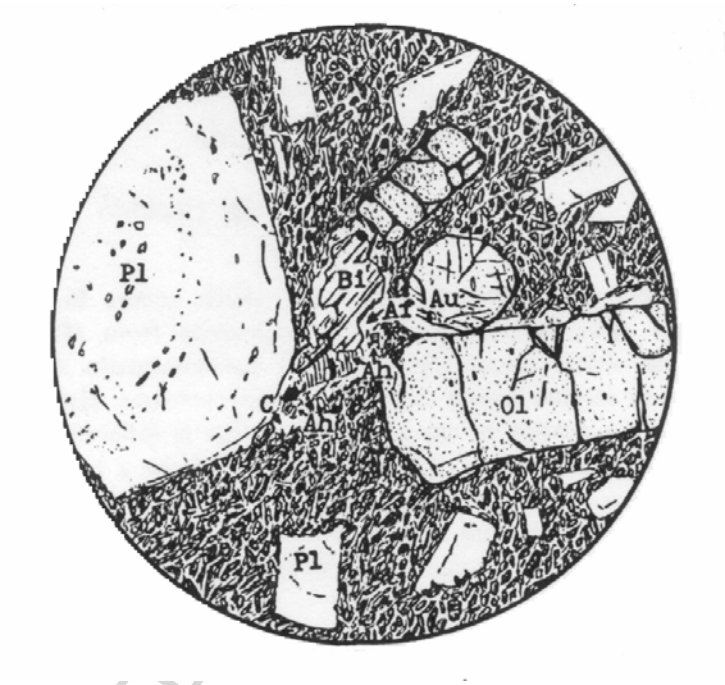

Luhr – Fig. 2

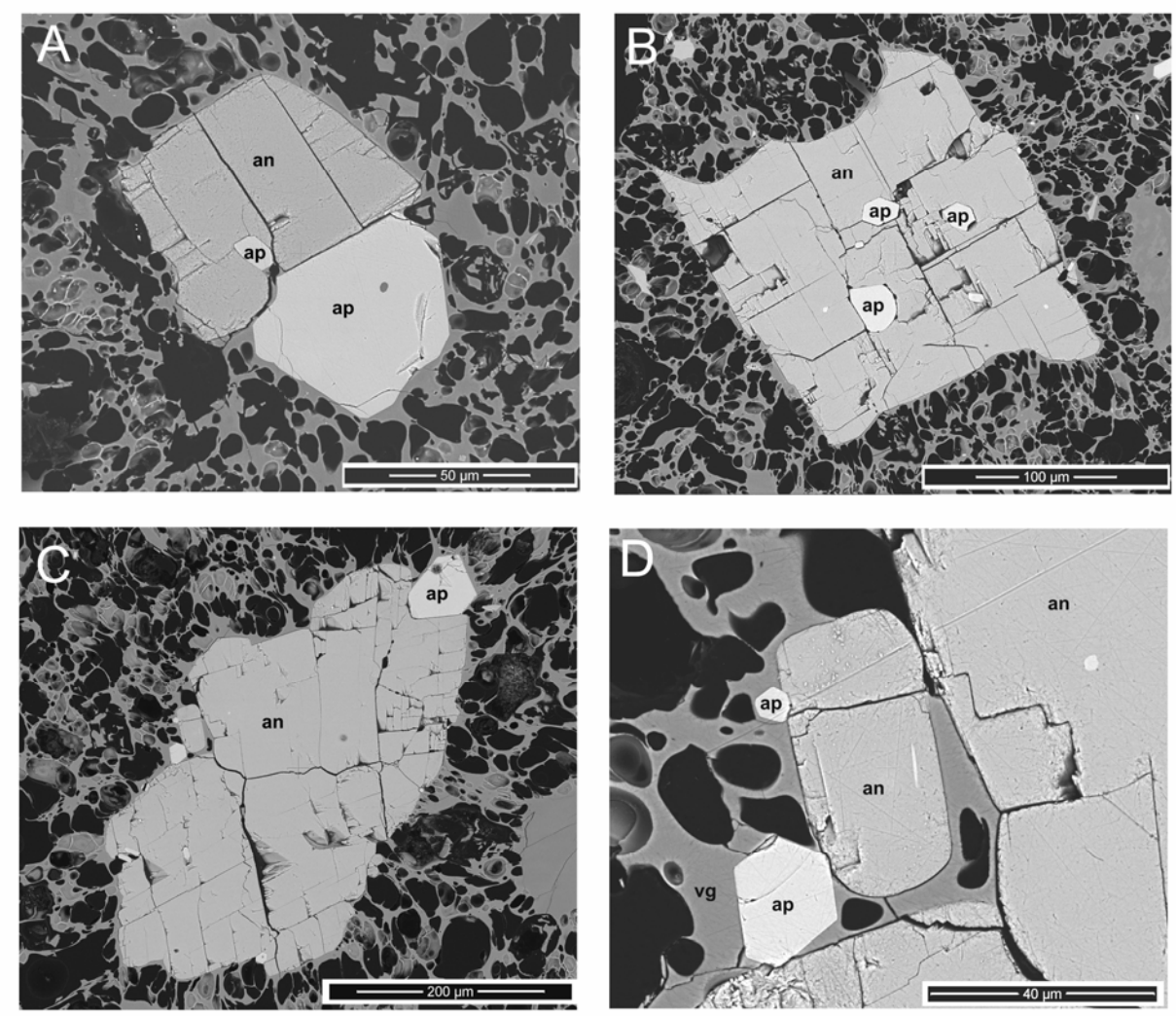

Luhr – Fig. 3

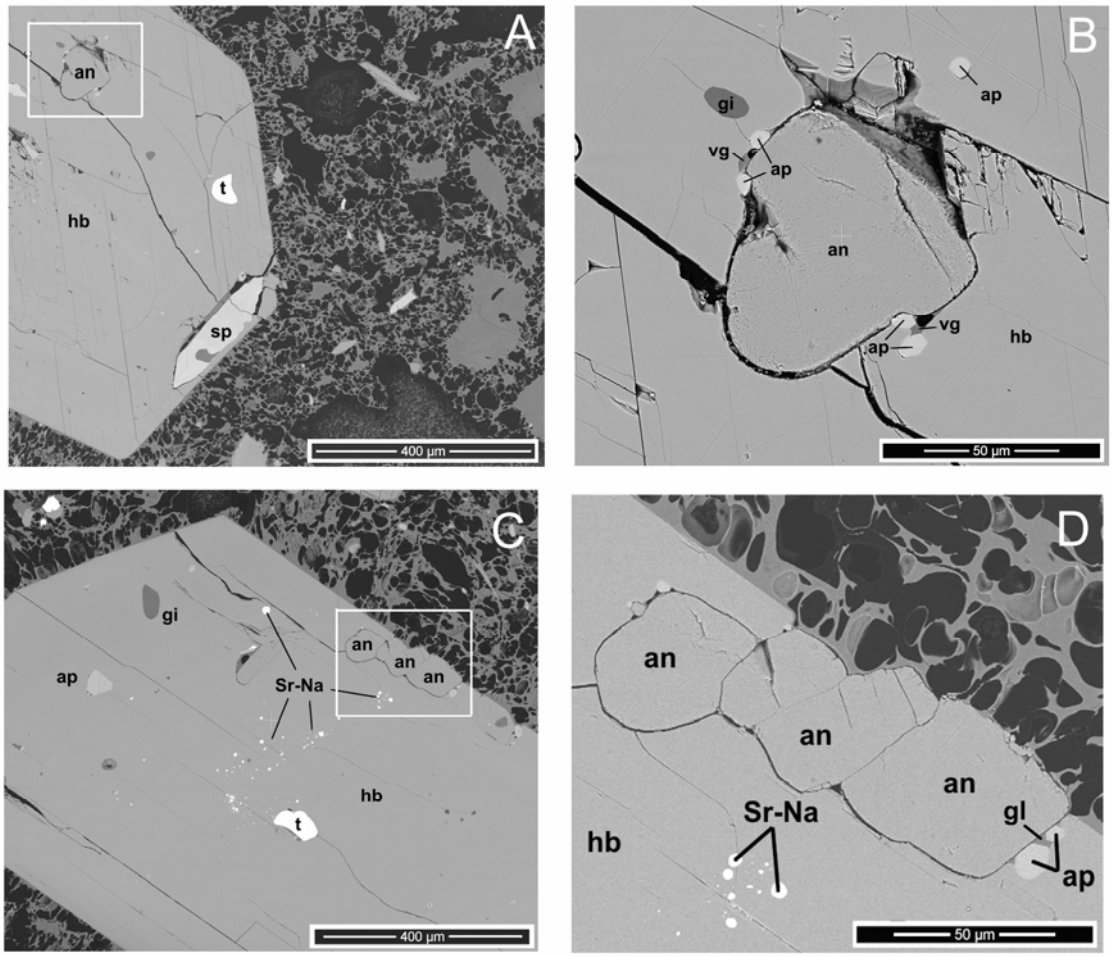

Luhr – Fig. 4

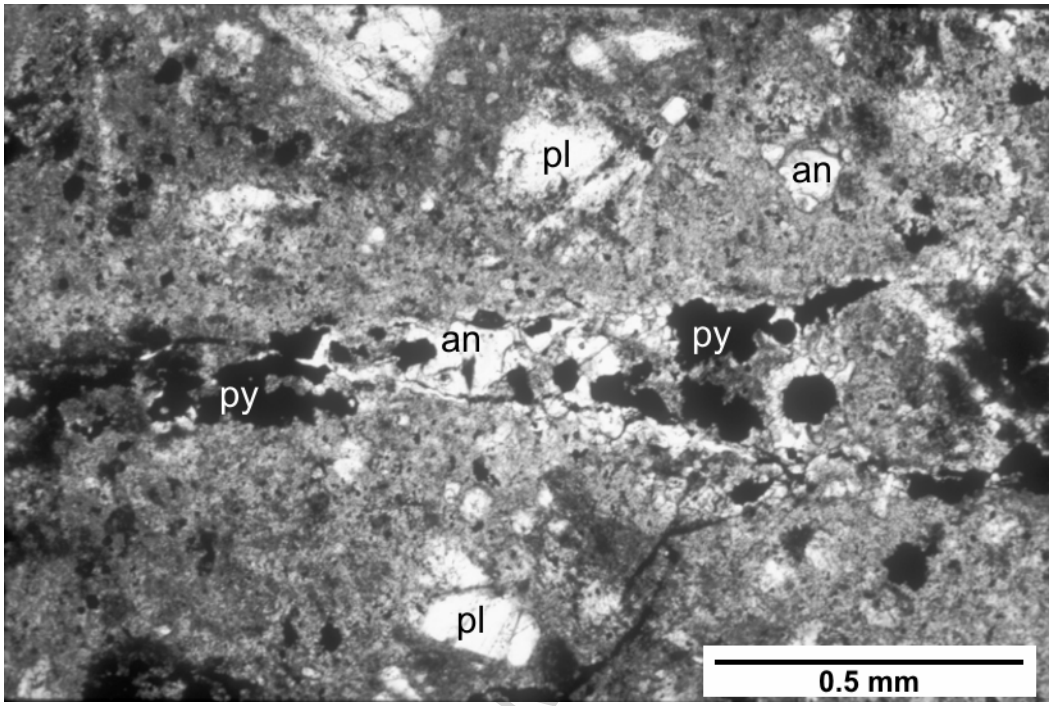

Luhr – Fig. 5

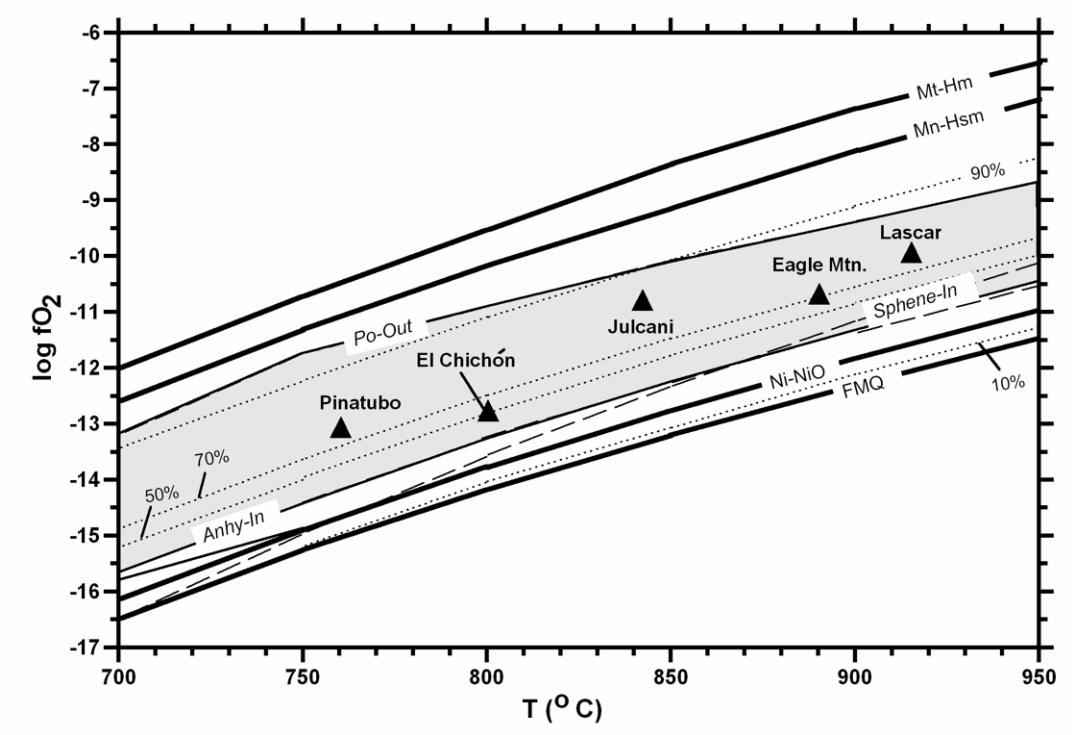

Luhr – Fig. 6

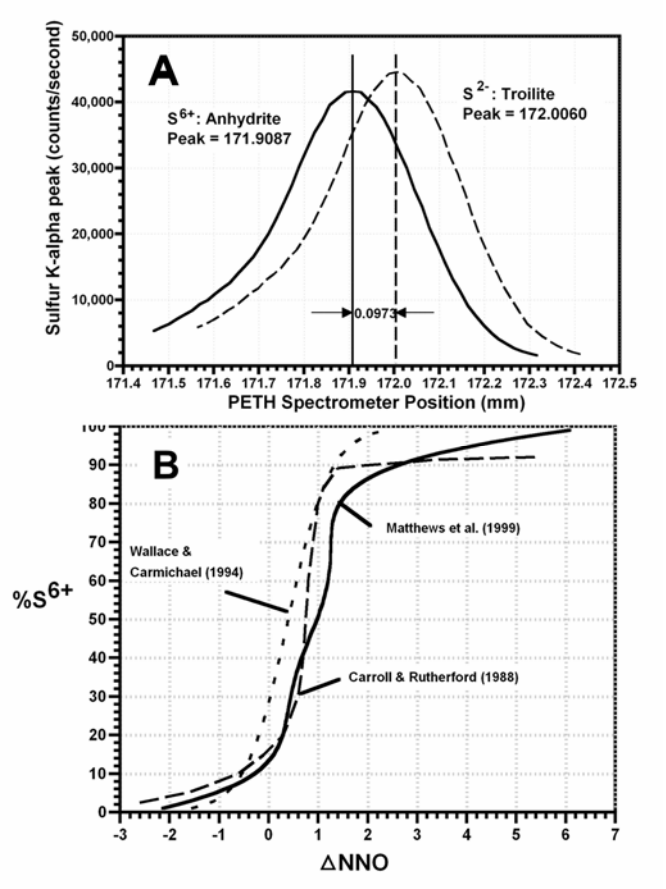

Luhr – Fig. 7

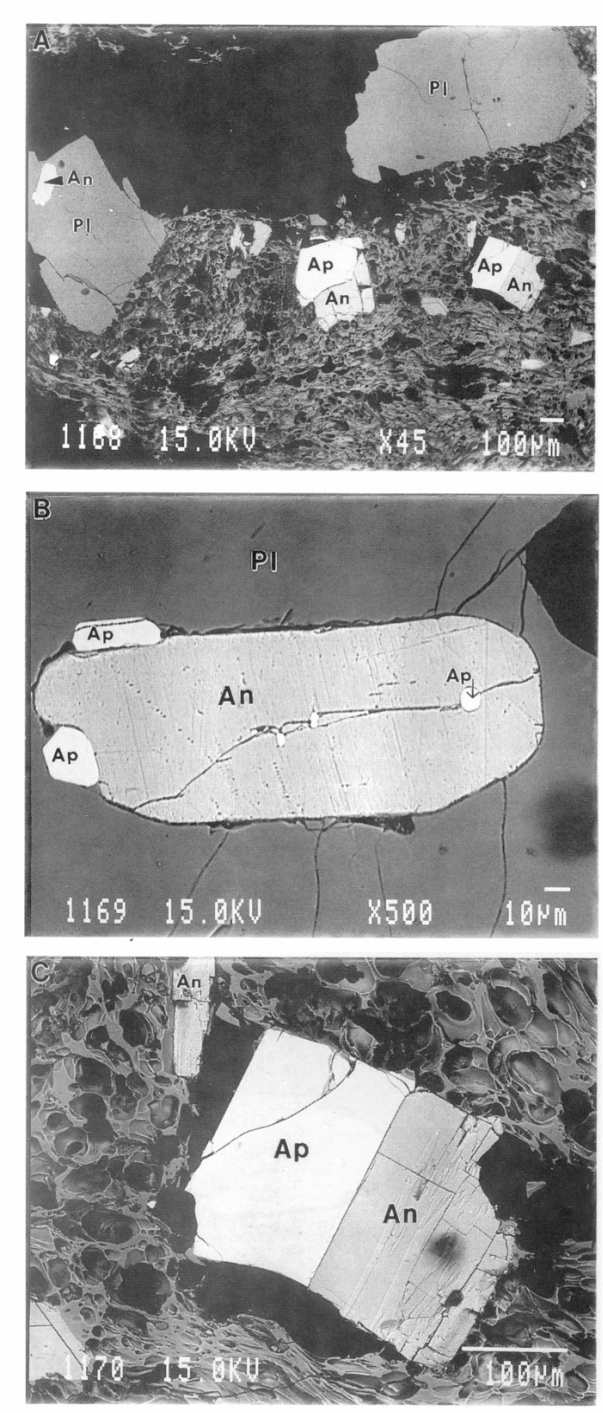

Luhr – Fig. 8

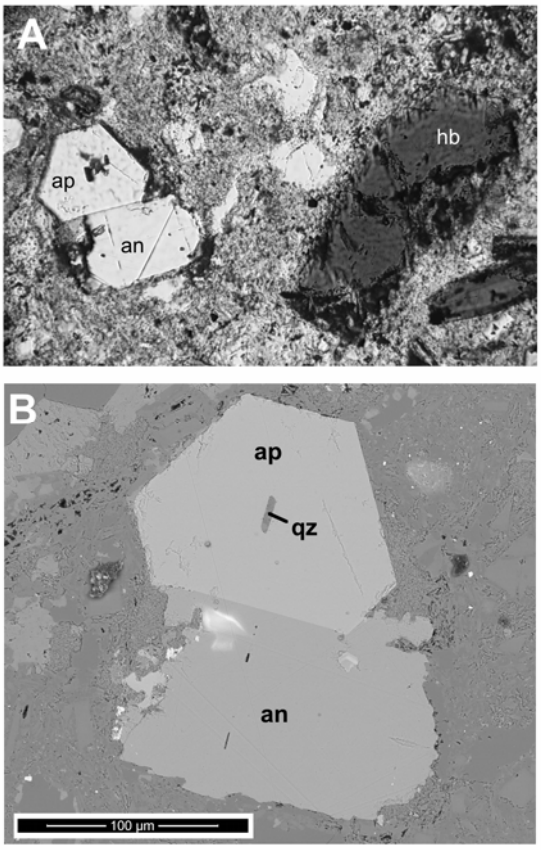

Luhr – Fig. 9

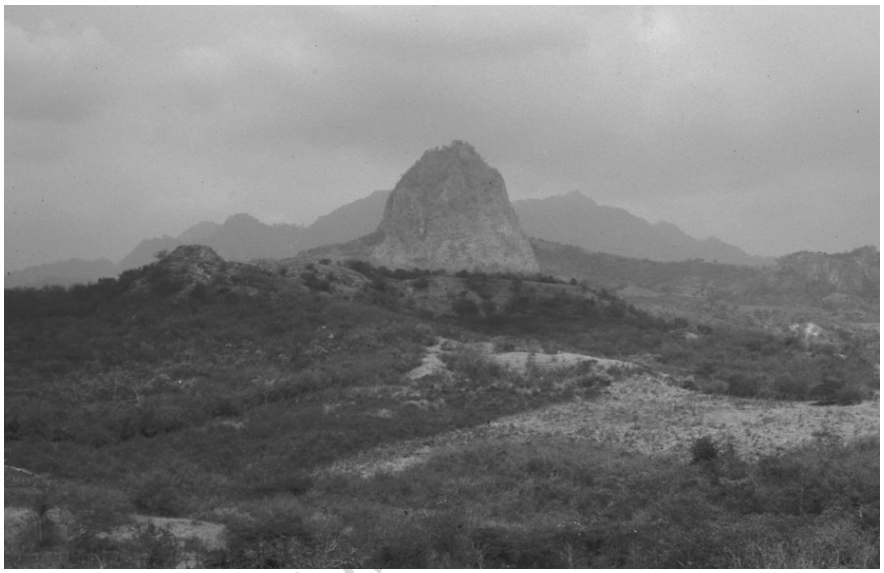

Luhr – Fig. 10

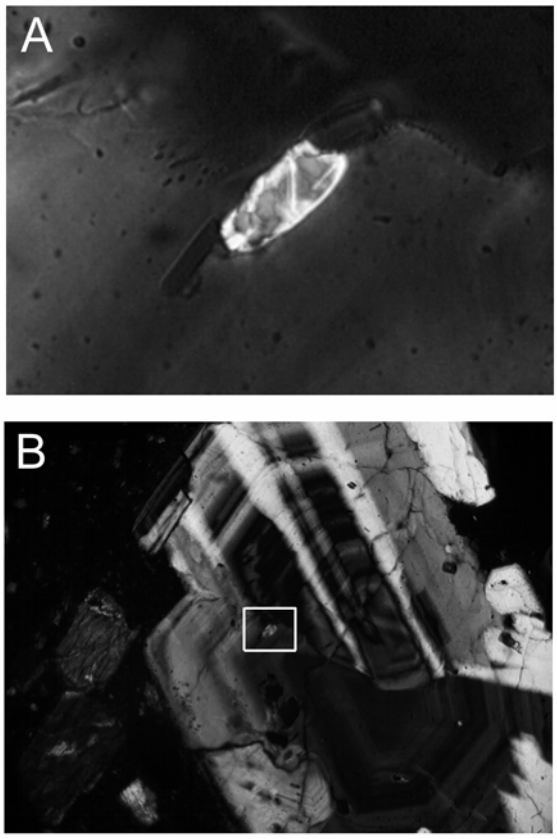

Luhr – Fig. 11

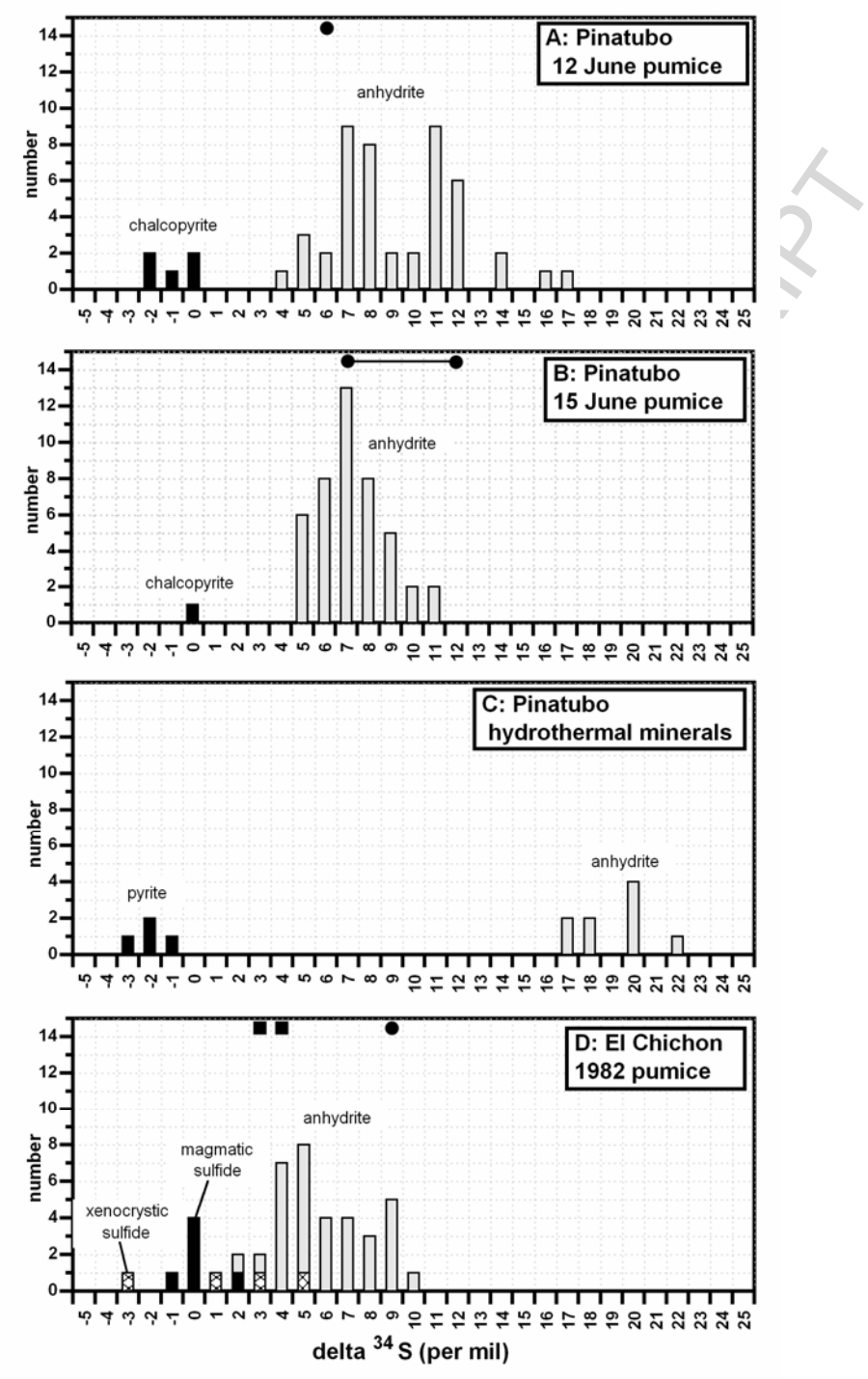

Luhr – Fig. 12